GEOCHEMISTRY, MINERALOGY AND PETROLOGY • SOFIA
ГЕОХИМИЯ, МИНЕРАЛОГИЯ И ПЕТРОЛОГИЯ • СОФИЯ
2010, **48**, 1-37.

The Sakar batholith – petrology, geochemistry and magmatic evolution

Borislav K. Kamenov, Vassil Vergilov†, Christo Dabovski, Iliya Vergilov, Lyudmila Ivchinova†

Abstract. Based on a new sample set and extensive re-mapping an attempt is made to elucidate the field relations, mineral composition, nomenclature, geochemical features, magmatic and postmagmatic evolution, and to find new evidence for geodynamic reconstructions of the Sakar batholith.

The dome-like batholith is emplaced into high-grade metamorphic rocks of still unclear age. It is covered by Permian and Triassic sedimentary rocks. The batholith is composed of the following granitoid units: equigranular in the inner parts, porphyroid with large microcline megacrysts in the outer parts, and small aplitoid bodies. Large xenoliths of gneisses and orthoamphibolites occur in the marginal parts of the batholith. The modal petrographic species are quartz-monzodiorite, quartz-monzonite, granodiorite, granite, quartz-syenite and leucogranite.

The main rock-forming minerals are separated from artificial heavy concentrates and studied optically, chemically, by X-ray and IR-analysis. No characteristic differences are observed for the plagioclase composition in the equigranular and porphyroid granitoids – An_{30}-An_{10}, but plagioclases in the aplitoid granitoids are more acid – An_{15}-An_{10}. Potassium feldspars are high microclines. Their rims are poorer in Sr, Ba, Li, Co and richer in Th and U. Biotite is a common variety with prevailing siderophyllite isomorphism. Muscovites are primary magmatic and secondary postmagmatic.

Based on 147 new analyses for 36 elements, some specific petrochemical and geochemical features are revealed and arguments in favour of primary and secondary petrogenetic evolution are discussed. Crystal fractionation is required to explain the geochemical pattern of the rocks. Late-magmatic to post-magmatic re-crystallization is supposed for the microcline porphyry crystals. The rocks are typically calc-alkaline and exhibit *REE* distributions intrinsic to plate margin orogenic settings. Mixed volcanic-arc and post-collisional discriminations argue for the presence of mantle component in the magma source and crustal contamination of the magmas. Presumably, melting of amphibolite/basaltic rocks from the lower crust could generate the parental magmas, which produced the rocks of the batholith by differentiation, fluid input and postmagmatic reworking.

Key words: Sakar batholith, mineralogy, petrology, geochemistry, magma evolution

Addresses: B.K. Kamenov, V. Vergilov, I. Vergilov, L. Ivchinova - Department of Mineralogy, Petrology and Economic Geology, Faculty of Geology and Geography, Sofia University, 1504 Sofia, Bulgaria; E-mail: kamenov@gea.uni-sofia.bg; Ch. Dabovski – Geological Institute, Bulgarian Academy of Sciences, 1113 Sofia, Bulgaria

Борислав К. Каменов, Васил Вергилов†, Христо Дабовски, Илия Вергилов, Людмила Ивчинова†. Сакарският батолит – петрология, геохимия и магматична еволюция

Резюме. Въз основа на нова съвкупност от проби и обширно полево прекартиране е направен опит за изясняване на полевите взаимоотношения, минералния състав, номенклатурата, геохимичните особености, магматичната и постмагматичната еволюция и са потърсени нови аргументи за геодинамичните реконструкции на Сакарския батолит. Куполоподобният батолит е вместен във високостепенни метаморфни скали с все още неясна възраст. Покрит е от пермски и триаски седиментни комплекси. Следните петрографски разновидности гранитоиди изграждат батолита: равномернозърнести във вътрешните части на тялото, порфироидни с крупни микроклинови мегакристали във външните части и аплитоидни в по-малки разкрития. Големи ксенолити от гнайси и ортоамфиболити се срещат в окрайните участъци. Модалните петрографски видове са кварц-монцодиорит, кварцмонцонит, гранодиорит, гранит, кварцсиенит и левкогранит.

Главните скалообразуващи минерали са сепарирани от изкуствени скални шлихи и са изучени оптично, химично, рентгеново и чрез ИЧ-анализ. Не са наблюдавани характерни различия в състава на плагиоклазите от равномернозърнестите и порфироидните гранитоиди – An_{30}-An_{10}, но плагиоклазите в аплитоидните гранити са по-кисели – An_{15}-An_{10}. Калиевите фелдшпати са висок микроклин. Техните периферни части са по-бедни на Sr, Ba, Li и Co и по-богати на Th и U. Биотитите са обикновена разновидност със сидерофилитов изоморфизъм. Мусковитите са първично магматични и вторични постмагматични.

Изследвани са петрохимични и геохимични проблеми и са изведени доводи за първичната и вторична петрогенетична еволюция с използване на 147 нови анализи за 36 елемента. Кристално фракциониране е привлечено за обяснението на новите геохимични данни за скалите, но късно-магматична до постмагматична прекристализация е предположената причина за образуването на фелдшпатовите порфироиди. Скалите са типично калциево-алкални продукти и редкоземните им разпределения са присъщи на орогенните обстановки от континенталните окрайнини. Смесени вулканско-дъгови и пост-колизионни дискриминации аргументират присъствие на мантиен компонент в магматичния източник и корово замърсяване на магмите. Вероятно топене на амфиболитови или базалтови скали от долната кора би могло да създаде родоначалната магма, която чрез диферен-циация, флуидно влияние и последваща постмагматична преработка е създала скалите на батолита.

Introduction

The Sakar batholith occupies the core of a large dome-like structure of high-grade metamorphic rocks. Considered as Caledonian (Boyanov et al. 1965), Hercynian (Dimitrov 1946; Dabovski 1968; Savov 1983; Arnaudov 1979; Dabovski & Haidutov 1980; Vergilov et al. 1986; Chatalov 1990), Late Jurassic (Skenderov et al. 1986) or Early Cretaceous (Ivanov et al. 2001) in age and interpreted as post-metamorphic, pre-metamorphic or syntectonic, the batholith still raises many unsolved problems concerning mainly the time of emplacement, the temporal relations emplacement/metamorphism/host rock deformations, its petrological evolution and geodynamic setting.

Brief information about the petrographic units, structural characteristics, emplacement mechanism, as well as the mineralogy and geochemistry of the batholith was presented in an extended abstract, including the main results of complex prospecting works in the area of Sakar Mts. However, the prevailing part of the collected then numerous new data remained unpublished (Vergilov et al. 1986[1]).

This paper aims to "revive" these unpublished data in the framework of a modern overview on the mineralogy, petrology and geochemistry of the Sakar batholith and to propose a model for its petrological evolution.

The field observations and the laboratory analyses were carried out between 1982 and 1986 when a geological map in scale of M 1: 50 000 was also compiled.

[1] Vergilov V, Kamenov BK, Ivchinova L, Vergilov I, Genov I, Dabovski C, Andreev A, Savov S, Haidutov I (1986). Petrology and structure of the Sakar Batholith, Lessovo type granites in the area of Radovets village and some intrusive bodies in the region east of Tundza River. Geoarchive of the Prospecting Enterprise of State company "Rare metals", Project 154/82, 371 p.

Abbreviations and symbols

Modal nomenclatures

Mgb	monzogabbro
Qmd	quartz-monzodiorite
Qmz	quartz-monzonite
Qsy	quartz-syenite
Mg	monzogranite
Lmg	leucomonzogranite
Slg	transitional leucogranite
Lg	leucogranite
Gr	granite
Sg	syenogranite
Gd	granodiorite
Gb	gabbro
D	diorite

Trends

◯	equigranular
△	porphyroid
◇	aplitoid

Series

TH	tholeiitic
CA	calc-alkaline
HKCA	high-potassium calc-alkaline
SH	shoshonitic
UKSH	ultra-high-potassium shoshonitic

Lessovo orthometamorphites

┼	metagranites
╳	metaquartz-diorites
▽	orthoamphibolites

Geological setting

The Sakar batholith is hosted into a high-grade metamorphic complex (Fig. 1) of ortho- and parametamorphic rocks, metamorphosed in Barrovian type amphiboilite facies (kyanite-sillimanite subfacies). They are unconformably overlain by Permian (?) and Lower-Middle Triassic metasediments.

The high-grade metamorphic complex in Sakar area has been for a long time subject of debate concerning its lithologic subdivision, age of the protholith and of the metamorphic overprint. In general, two different concepts have been proposed.

According to the widely accepted ideas of the last century and the 1:100 000 Geological Map of Bulgaria (Kozhoukharov et al. 1994, 1995), the metamorphic rocks are assigned to the so-called Pra-Rhodopian Supergroup. It is subdivided into two groups (Strazhets and Boturche) and the latter – into several litho-stratigraphic units. The lower Strazhets Group consists of leptite-gneisses, porphyroblastic gneisses and gneisses, and the upper Boturche Group – of gneisses, gneiss-schists and schists with intercalations of metaquartzites, amphibolites and metamorphosed ultrabasic (metapyroxenites, metagabbro) rocks. The age of the protholith and of the amphibolite facies metamorphic event is assumed to be Precambrian. In this scheme the Sakar pluton was emplaced during the Upper Paleozoic, i.e. is post-metamorphic.

A recent model (Gerdjikov & Ivanov, 2000; Ivanov et al. 2001; Gerdjikov 2005) advocates another concept – the protolith of the high-grade metamorphic rocks in Sakar Mts. is a continuous sedimentary-volcanogenic succession of Late Paleozoic–Early Mesozoic age that was deformed and metamorphosed in amphibolite facies in Late Jurassic–Early Cretaceous time. The Sakar pluton was emplaced in this parametamorphic complex approximately during the same time span as a synkinematic intrusion.

The *parametamorphic complex* in the southern exocontact zones of the batholith is affected by periplutonic migmatization (Fig. 1) in narrow zones of more abundant foliation-parallel and cross-cutting aplitoid injections and potassium feldspar porphyroblastesis.

A special feature of the parametamorphic complex is the development of porphyroblastic large-flaked reddish-brown biotite, superimposed on the usual brown biotite of the metapelitic rocks (gneisses and paraamphibolites) even over the regressive mineral association (chlorite, calcite, muscovite, pale-green acicular amphibole, and epidote). Along with the large-scale irregular microclinization, this biotitization is understood as an exocontact effect of the granitoid magma.

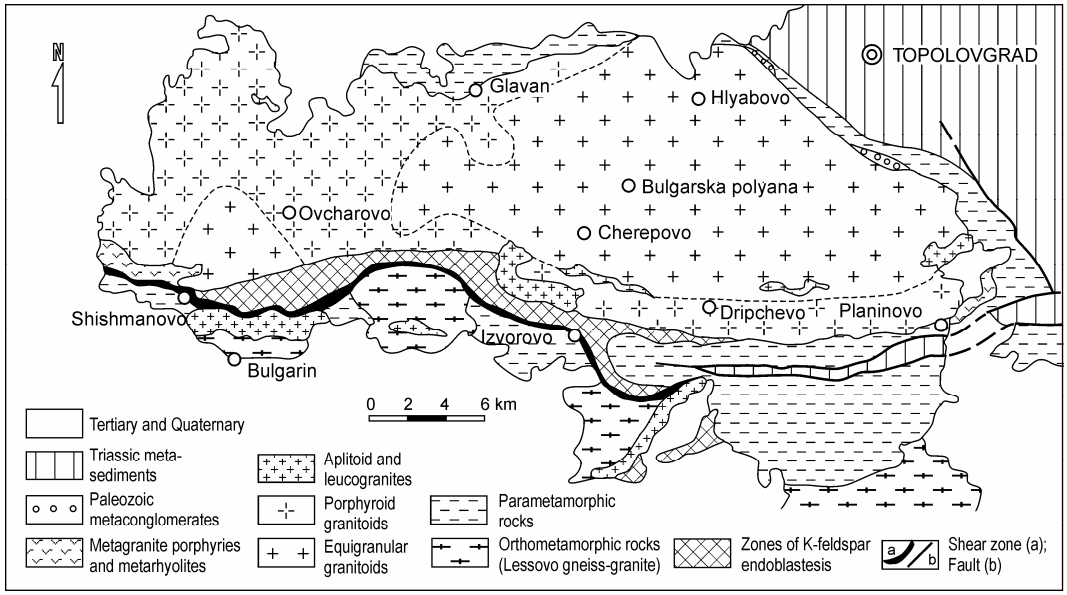

Fig. 1. Geological sketch map of the Sakar batholith (after Vergilov et al. 1986 and Ivanov et al. 2001)

The foliated granites emplaced within the metamorphic complex close to the southern margin of the pluton (Fig. 1) are referred to the *Lessovo orthometamorphic complex* (Kamenov et al. 1986). These rocks Ivanov et al. (2001) describe as "Sakar type" schistose granites of the so-called Izvorovo Dome. As a facial variety of the Sakar pluton, they were described also by Boyanov et al. (1965) and Dimitrov (1956, 1959). The idea of their Precambrian age was adopted by Savov (1983), Kozhoukharova & Kozhoukharov (1973), Kozhoukharov (1984a). Vergilov et al. (1986) assumed Late Paleozoic age. Dimitrov (1999) studied in detail the internal structure of the metagranitoids in the area of Radovets village.

Small bodies of metagranite porphyry and metarhyolite of the so-called *Melnitsa orthometamorphic complex* (Vergilov et al. 1986[1]) are exposed close to the southwestern and southeastern margin of the batholith (Fig. 1). The outcrops near Shishmanovo village were described by Ivanov (1964) and those east of Tundzha river valley – by Chatalov (1992). Permian age of these rocks seems most probable.

The high-grade metamorphic basement is unconformably covered by the rocks of *Tchernogorovo Formation* (Čatalov, 1961) of assumed Permian age (Kozhoukharov et al. 1968). The unit consists mainly of metamorphosed breccia-conglomerates, which contain pieces of metamorphic rocks, metaquartzdiorites of Lessovo type, aplitoid two-mica granites, equigranular granites of Sakar type and metarhyolites.

The overlying *Triassic terrigenous and carbonate sediments*, known as "Sakar type Triassic" (Chatalov, 1990), are metamorphosed in the lower-temperature staurolite-almandine subfacies of the amphibolite facies. They are subdivided into three lithostratigraphic units (Paleokastro, Ustrem, and Srem) of faunistically proven Lower–Middle Triassic age. The idea of Ivanov et al. (2001) that the parametamorphic, Paleozoic and Triassic sequences suffered equal-grade regional metamorphism remains only a hypothesis.

The published Rb/Sr radioisotope dating of the batholith is conflicting. The dates of 320±18 Ma (Zagorchev et al. 1989), 499±70

Ma (Lilov 1990), and 250±35 Ma (Skenderov & Skenderova 1995) are obtained from approximately the same bulk rock samples and their interpretation is problematic (see the discussion in Ivanov et al. 2001). Unconvincing are also the available K-Ar data, which range in the interval 144–111 Ma (Palshin et al. 1989; Skenderov et al. 1986; Lilov 1990; Boyadjiev & Lilov 1972; Firsov 1975). They reflect only a regional thermal event, but not the emplacement age of the granitoids. New U/Pb zircon dating of samples from the batholith (Georgiev et al. 2006) yields 306.3±2.7 Ma. They suggest Carboniferous crystallization age and are in accord with the age deduced from geological evidence – clasts of equigranular and porphyroid granitoids (resembling those of Sakar pluton) are observed in the metaconglomerates of Chernogorovo Formation (Permian?) and in the basal conglomerate of the Lower Triassic Paleokastro Formation. From this viewpoint the idea of Ivanov et al. (2001) that the Sakar pluton was emplaced at least after the end of the Middle Triassic seems for the time being ill-founded.

Materials and method

The rock-forming minerals are examined in thin sections optically and in monomineral fractions, separated from 14 bulk rock samples for artificial heavy concentrates, representative for all rock varieties (Fig. 2). Moreover, large porphyroids of potassium feldspar are picked out by hand and some of them are analyzed chemically, separately for their internal cores and rims. The separation of the samples is done in the Department of Petrology of Sofia University with the methodical assistance of V. Arnaudov. X-ray measurements are on difractogrammes, obtained in DRON-2 and TUR M62 instruments. Filtered Co-rays are used and chemically pure NaCl for internal standard is applied. The IR-spectra are made on spectrometer IR-20 using standard methods in pressed pallets. The instrument is calibrated with the frequency of the absorption bands of the 1, 2, 4-trichlorbenzen. 14 samples of plagioclases and 41 of potassium feldspars are processed and their X-ray and IR-ordering degrees are calculated.

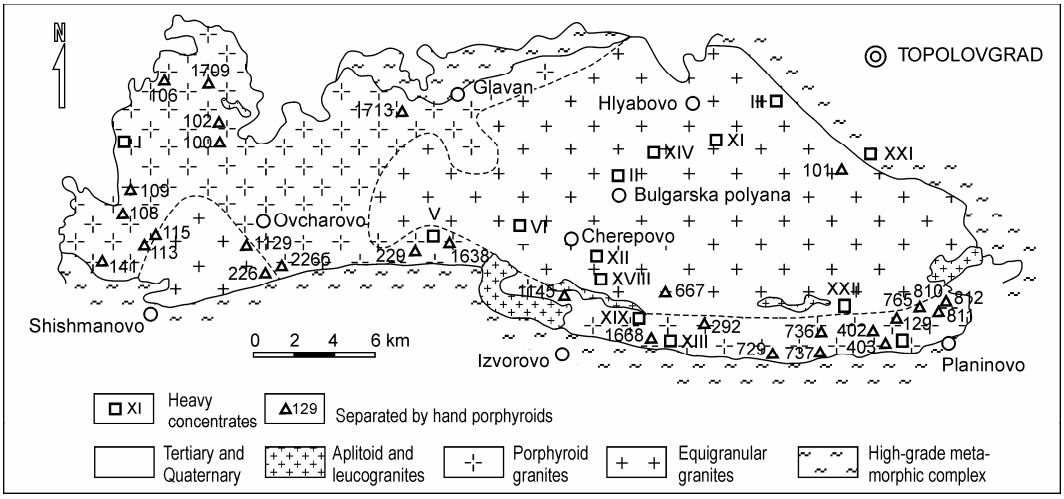

Fig. 2. Sketch showing sample location of artificial heavy concentrates and microcline porphyroids separated by hand

The geochemical results are based on 147 silicate assays on rock samples and on 64 analyses on rock-forming minerals (plagioclases – 12, potassium feldspars – 40, biotites – 10 and muscovites – 2) performed by the classical wet method in the Chemical Laboratory of the Department of Petrology under the guidance of L. Ivchinova. 110 rock samples and 64 monomineral samples are analyzed by XRF in the Geological Institute at the Bulgarian Academy of Sciences under the guidance of G. Panayotov for determination of Ba, Sr, Zr, Rb, V, Ti and Mn; by INAA in the Laboratory of the former Geological Survey under direction of Z. Tchoubriev for the elements Th, U, Hf, Ta, Cr, Sc, Au, Co, Cs, La, Ce, Sm, Eu, Tb, Yb, Lu and Au and by AAS in the Faculty of Geology and Geography, Sofia University executed by E. Landjeva for the elements Zn, Cu, Ni and Li.

Petrography

The Sakar pluton is a dome-like granitoid body of batholithic size elongated in east-west direction – its long axis is about 20 km and the width is between 7 and 15 km. The dome structure is outlined by planar flow structures of biotite, microcline and flattened xenoliths as well as by mineral lineation (Dabovski & Haidutov 1980; Vergilov et al. 1986). Most often the contacts are sharp and intrusive but conformable to the foliation in the host rocks. Numerous aplite veins and some basic dykes cut the plutonic rocks. The degree of preferred orientation of the magmatic inclusions, xenoliths and phenocrysts increases towards the marginal porphyroid facies, whereas the internal parts of the pluton are almost structureless. The increasing degree of deformation toward the contact zones supports the idea of "balloon mechanism" of emplacement.

Three petrographical units compose the pluton: (1) equigranular granitoids, outcropping in the internal parts along the crest of Sakar Mountain, (2) porphyroid on the microcline granitoids and (3) aplitoid leucogranites, occurring mainly in the peripheral parts of the pluton. The transitions between the units are gradual and only the aplitoid leucogranites have sharp contacts. The advanced assimilation of amphibolite packets from the host rocks leads to appearance of mesocratic granitoids containing much more biotite. The granitoids around gneiss xenoliths become richer in muscovite and acquire schistose structure. Magmatic mafic inclusions are also observed. The porphyroid granitoids occupy large areas in the northwestern, western and southern marginal parts of the batholith. The mineral composition of the porphyroid and equigranular granitoids is qualitatively equal. The difference is only in the content and size of microcline.

The modal relationships of the major rock-forming minerals (Fig. 3) show that the equigranular granitoids are quartz-monzodiorite, granodiorite and monzogranite, the last being the prevailing nomenclature. Almost the same is the modal composition of the porphyroid granitoids, but granodiorites predominate and, instead of quartz-monzodiorite, there are single cases of quartz-monzonites. The relatively more basic varieties are richer in femic minerals and occur in the mesocratic contaminated rocks around amphibolite xenoliths. The aplitoid granitoids plot in the fields of the granodiorites and mainly of the monzogranites, but individual specimens are even quartz-syenites and granosyenites. A characteristic feature of these rocks is their poorness in femic minerals – a good reason for naming them leucogranites. The main trends of the three rock units suggest some differences in their conditions of formation. The main trend in the equigranular rocks (trend 1 in Fig. 3) is connected with a process of synchronously increasing modal contents of quartz and alkali feldspars. Trend 2 in the porphyroid granitoids is disturbed and deformed by the late- to post-magmatic microcline recrystallization and is indicative for increasing quartz quantities at relatively constant ratio plagioclase/alkali feldspars. Trend 3 in the aplitoid granitoids follows mainly the variation direction of the alkali feldspars/plagioclases ratios.

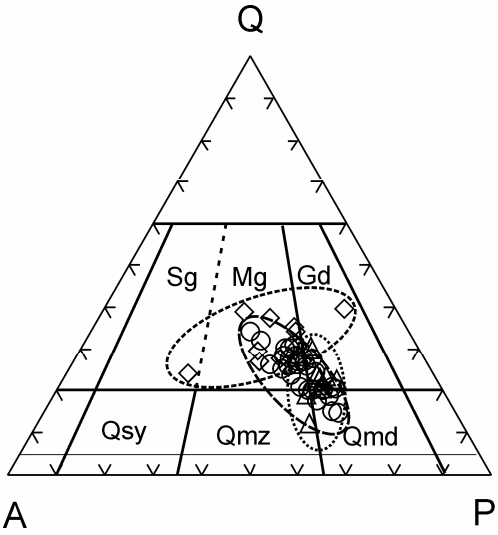

Fig. 3. APQ classification diagram for modal analyzed rocks from the Sakar batholith

Massive coarse-grained structure of the rocks is most commonly observed, but parallel orientation of micas, feldspar porphyries and xenoliths in the marginal parts of the batholith is also typical. Some indications of later re-orientation are registered in these areas. The monzonitic texture of the rocks is usually combined with myrmekite and perthite symplectites. Micrographic intergrowths of microcline and quartz are also found in the aplitoid granites. The sequence of crystallization is generally plagioclase–biotite–quartz–allanite–potassium feldspar.

The xenoliths in the batholith consist of amphibolites and gneisses. They can be met almost everywhere, being most abundant in the marginal parts of the batholith. Showing conformable orientation with the metamorphic schistosity of the host rocks, they are nearly parallel to the primary planar flow structures and it seems as if they form a semi-transparent "ghost" dome-like structure, similar to the real dome-like shape of the batholith. The packets of gneisses are granitizated and their boundaries with the granitoids are gradual. The granitization of the mafic xenoliths leads to the development of biotite and amphibole, sometimes to increasing quartz quantity or to appearance of rare large microcline crystals. The amphiboles associate with rutile followed by titanite. The extreme result of the process is the transformation of the orthoamphibolites into amphibole-biotite and biotite gneisses, rich in titanite. Typical magmatic textures are preserved in the weakly metamorphosed metabasites.

Mineral composition

Plagioclase. Two morphological types of plagioclases are distinguished in the equigranular and the porphyroid granitoids: a coarse-grained and fairly euhedral (Pl^{I}) and a fine-grained and isometric one (Pl^{II}). The coarse-grained plagioclase is prismatic and usually no polysynthetic twinning is observed or the twinned lamellae are a few or indistinct. The anorthite composition of Pl^{I} is An_{30}-An_{10} and more often with uniform variation in the range An_{26}-An_{15}. Plagioclases of blurred zoning are also found in the central parts of the batholith – An_{30} in the cores and An_{22} in the rims of the crystals. Sometimes thin edges of nearly pure albite (An_{10}-An_{5}) coat the plagioclases. Usually the crystals of this generation are overfilled by alteration products mostly muscovite and epidote. The second generation plagioclase is clean of secondary minerals. It occurs in aggregates together with fine-grained microcline and quartz. It should be noted that almost everywhere Pl^{II} shows reversed zoning. Its anorthite composition is of narrow range – An_{23}-An_{20} in the cores and An_{27}-An_{25} in their rims. No essential differences between the contents of the trace elements Sr, Ba, Rb, Zr and Li in the equigranular and porphyroid granitoids are established (Table 1). The IR-spectra of plagioclases were examined applying the method of Plyusnina & Hachatrjan (1980) to estimate their anorthite composition and structural ordering degree. The coincidence with the results of other methods is good and the prevailing ordering degree corresponds totally to partly ordered plagioclases.

Table 1. *Chemical composition of representative plagioclases from artificial heavy concentrates from Sakar batholith*

Granitoids	Equigranular			Porphyroid	Aplitoid	
Sample	S-V	S-XIV	S-XII	S-XIII	S-XVIII	S-IX
Analysis	Pl-1	Pl-2	Pl-3	Pl-4	Pl-5	Pl-6
SiO_2	65.61	68.14	68.51	64.20	64.31	71.95
TiO_2	0.08	0.12	0.16	0.12	0.15	0.12
Al_2O_3	19.80	17.59	17.50	20.88	20.76	15.98
Fe_2O_3	0.58	0.27	0.32	0.35	0.45	0.35
FeO	0.15	-	-	-	-	0.18
MnO	0.006	0.006	0.006	0.007	0.02	0.003
MgO	0.27	0.15	0.42	0.28	0.31	0.34
CaO	3.46	3.10	2.93	4.99	4.93	1.10
Na_2O	7.40	5.57	5.58	6.73	6.65	6.83
K_2O	1.70	3.82	3.32	1.89	1.59	2.12
P_2O_5	0.38	0.04	0.09	-	-	0.12
H_2O^-	0.04	0.18	0.16	0.07	0.05	0.06
H_2O^+	0.40	0.53	0.55	0.16	0.33	0.37
Total	99.87	99.52	99.55	99.68	99.55	99.52
Sr	429	427	437	630	678	166
Ba	203	929	934	730	470	113
Zr	28	68	87	10	10	50
Rb	45	140	125	60	28	55
Li	7	15	15	13	5	5
An	18.3	17.5	17.2	25.7	26.2	6.9
Ab	70.9	56.9	59.5	62.7	63.8	77.3
Or	10.8	25.6	23.3	11.6	10.0	15.8

The plagioclases of the aplitoid granitoids are not altered and their composition is a bit more acid – An_{20}-An_{10}. They are fine-grained and polysynthetically twinned. According to the IR-data they have preserved their partial structural disorder.

Superimposed irregular albitization on the primary composition of the plagioclases is locally observed. In particular cases, as for example south of Orlov Dol village, the albitization has spread over larger areas and has obliterated the primary magmatic twinning.

Microcline is developed in all rock varieties of the pluton. The large-sized crystals reach to 10–12 cm in the porphyroid unit. They are white in colour, have low contents of iron oxides and contain poikilitic inclusions of plagioclase, quartz and rarely biotite. Everywhere the microcline exhibits cross-hatching and very often perthitic exsolutions are noted. Myrmekitic textures and outer envelopes of albite are observed. The measured value of the angle $2V_x$ on single crystals is between 81^o and 87^o. X-ray and IR-data of separated monomineral samples of K-feldspars are shown in Table 3. It is noteworthy that the admixtures of plagioclase, included into the porphyries, cannot be separated perfectly from the exsoluted perthitic albite and that is why the calculated albite component in the potassium feldspars is slightly higher. It concerns chiefly the porphyroid granitoids. The K-feldspars are more contaminated with quartz inclusions and show higher albite components, as well as hematite products in theirs outer parts, whereas more apatite accessories are observed in their internal cores. This hampers the correct estimation of the bulk chemical composition of the feldspars. An attempt is made to estimate the proportion between the isomorphic albite component in the microcline porphyries and the mechanically included in

Table 2. *Chemical composition of selected potassium feldspars*

Granitoids	Equigranular			Porphyroid					AGr
Sample	V	XIV	XII	115в		113		108	XVIII
Analyses	KFd1	KFd2	KFd3	KF-c	KF-r	KF-c	KF-r	KF10	KF11
SiO_2	63.92	62.77	63.93	63.59	63.73	64.51	68.18	64.34	63.92
TiO_2	0.04	0.04	0.04	0.07	0.09	0.92	0.19	0.12	0.05
Al_2O_3	17.77	18.63	17.47	18.37	18.50	18.15	15.90	18.14	18.08
Fe_2O_3	0.28	0.37	0.15	0.73	0.57	0.52	1.23	0.65	0.21
FeO	0.09	-	-	0.12	0.14	0.15	0.27	0.23	0
Mn*	15	140	40	0.01	0.01	0	0	0	0.005
MgO	0.20	0.37	0.17	0.34	0.32	0.30	0.52	0.31	0.37
CaO	0.37	1.01	1.07	0.26	1.04	1.00	1.40	1.38	1.09
Na_2O	1.17	1.26	1.59	2.88	2.72	3.20	3.05	3.00	1.47
K_2O	15.94	14.43	14.26	12.30	12.22	11.43	8.34	11.95	14.24
P_2O_5	0.07	0.06	0.06	0.10	0.16	0.02	-	0.26	-
H_2O^-	0.08	0.23	0.13	-	-	-	-	0.05	0.13
H_2O^+	0.08	0.87	0.60	0.27	0.35	0.35	0.60	0.32	0.44
Total	100.01	100.05	99.47	100.04	99.83	99.75	99.68	100.10	100.01
Sr	348	401	440	493	479	387	284	519	534
Ba	2663	4370	4900	4102	4041	3883	2365	4258	7190
Zr	P20	<20	25	<20	<20	37	56	23	<20
Rb	381	623	490	222	204	299	233	276	285
Li*	30	110	25	20	20	18	15	20	20
Cs	3	38.7	3.5	0.8	1.0	1.7	4.8	1.9	1.2
Th	0.4	1.2	2.0	1.0	1.0	2.8	8.5	2.7	0.6
U	0.2	0.6	0.9	0.5	0.6	2.0	4.5	1.0	0.2
Hf	-	0.5	0.9	0.4	0.6	0.7	1.9	0.6	0.1
Ta	-	10.2	0.1	0.2	0.1	0.5	1.2	0.1	0.1
Sc	0.1	0.1	0.2	0.2	0.4	0.6	1.5	0.6	0.2
La	1.5	3.6	7.5	3.4	3.9	6.6	16.2	16.0	1.3
Ce	2.1	5.2	12.0	6	8	9	21	23	3.1
Sm	0.1	0.6	1.2	0.4	0.5	1.3	3.6	1.5	0.2
Eu	0.6	0.4	0.2	0.35	0.63	1.22	0.77	1.44	0.3
Tb	-	-	0.1	-	-	0.3	0.8	0.1	-
Yb	-	2.2	0.2	-	0.1	0.5	1.2	0.2	-
Lu	0.01	-	0.09	-	-	0.18	0.44	0.03	-
Or %	99	85.3	84.3	78	75	70	62	77	84
Ab %	1	6.7	10.5	21	22	28	32	21	10
An %	0	2.6	0	1	2	2	6	11	1
Quartz %	0	0	0.3	0	0	0.4	1.5	1	0
Purity %	95	95	95	94	96	96	80	96	95

AGr – aplitoid granitoids

them plagioclase using the 201 reflexes ratio of the microcline and the albite, located at about 21^o and 22^o ($2\theta_{Cu}$). The albite component in microclines, estimated by X-ray data, is less than 10 mol% in all analyzed microclines. Within the framework of the accuracy it corresponds well to the chemically determined bulk sodium content in microclines from the equigranular granitoids. On the contrary, in the porphyroid granitoids where the large porphyries are picked out by hand, the difference is significant. There the average chemically analyzed content of the albite component is 25.1%, whereas the X-ray data

Table 3. *Phase composition, Al-sites in the crystallographic cell, structural ordering degree of selected monomineral potassium feldspars, according to chemical, X-ray and IR-analyses*

Granitoids		Equigranular					Porphyroid					AGr
Samples		S-V	S-XIV	S-XII	S-II	S-III	296	226	229	667	765	XVIII
Composition from silicate analysis %	Or	99.0	85.3	84.3	86.2	94.0	66.0	54.3	75.9	78.7	76.2	84.0
	Ab	1.0	6.7	10.5	11.1	9.5	24.4	45.4	17.1	15.6	5.8	10.0
	An	0.0	2.6	0.0	0.0	0.5	8.0	0.3	-	5.7	7.6	6.0
Composition from X-ray analysis 2θCu	Or in KF	100.00	68.80	83.20	88.00	100.00	66.20	51.00	76.00	85.00	96.90	94.90
	Ab in KF	6.00	8.00	8.80	4.00	8.00	0.20	8.00	2.00	4.00	7.60	9.60
	T1O	0.955	0.934	0.934	0.934	0.955	0.913	0.935	0.865	0.885	0.920	0.901
	T1m	0.045	0.03	0.032	0.027	0.019	0.053	0.025	0.035	0.055	0.028	0.009
	T2O=T2m	0.000	0.018	0.017	0.047	0.013	0.017	0.020	0.050	0.030	0.026	0.045
	Δp	0.89	0.88	0.87	0.91	0.9	0.83	0.95	0.83	0.8	0.87	0.86
Ordering degree from IR-analysis	Δ_{IR}	0.92	0.98	0.95	0.94	0.83	0.95	1.00	1.00	1.00	0.92	0.98
Purity in per cent		95	95	95	97	94	90	99	93	94	92	95

gave 3.2%. This means that at least 20% of the chemically analyzed albite component owes its value to the monzonitic plagioclase inclusions and that the isomorphic albite component before the exsolution of the perthites was lower than that of the microclines in the equali-granular granitoids.

The ordering degree of Al and Si in the tetrahedral sites of the potassium feldspars is calculated using the splitting of the reflexes 131 and 131 (Laves & Goldschmidt 1956) and the statistical occupancy of Al in the four possible crystallographic sites in the cell – by the method of the "three peaks" (Wright 1968; Stewart & Wright 1974). The IR-ordering degree is obtained by means of the frequency difference in the bands 650 cm^{-1} and 550 cm^{-1} after Kouznetsova (1970) and Kouznetsova et al. (1974). All samples are with split reflexes $2\Theta_{131-131}$ and show essential differences in the contents of Al in the sites T_1O and T_1m. Hence, the potassium feldspars are represented only by a triclinic high microcline. A systematic decrease in the content of Al in the site T_1O is established in the sequence equigranular (average 0.942) – porphyroid (average 0.905) – aplitoid (0.901) granitoids. A valid reason for this specific feature is the relatively quicker crystallization in the peripheral parts of the pluton, as well as the smaller size of the aplitoid granite bodies. We must not discount the role of increasing fluid pressure in the final stages of the growth of the porphyries.

Microclines of the Sakar batholith have similar structural characteristic as those from the so-called "Sredna Gora granitoids" or the "Rila and Rhodope granitoids" (Arnaudova et al. 1981; Arnaudova & Arnaudov 1982; Sarafova 1966; Grancharov et al. 1981; Arnaudova et al. 1990).

The average contents of Rb in the potassium feldspars (in ppm) from the batholith decrease in the following direction: equigranular (497, n=5) – porphyroid (335, n=35) – aplitoid (285, n=1) granitoids. Still lower are the average Rb contents in microcline from pegmatite – 252 ppm. These figures differ considerably from the published data for the potassium feldspars from Rila and Sredna Gora areas (225, n=5) and also from the Rhodope type granitoids (290, n=41), but they are approximately of the same order as the feldspars from Osogovo (460, n=3) and Pirin (390, n=6) granitoids (Arnaudova & Arnaudov 1982).

The correlations between Rb concentration in the rocks and in their feldspars (Fig. 4a) indicate different conditions of formation in both rock units – negative correlation for the

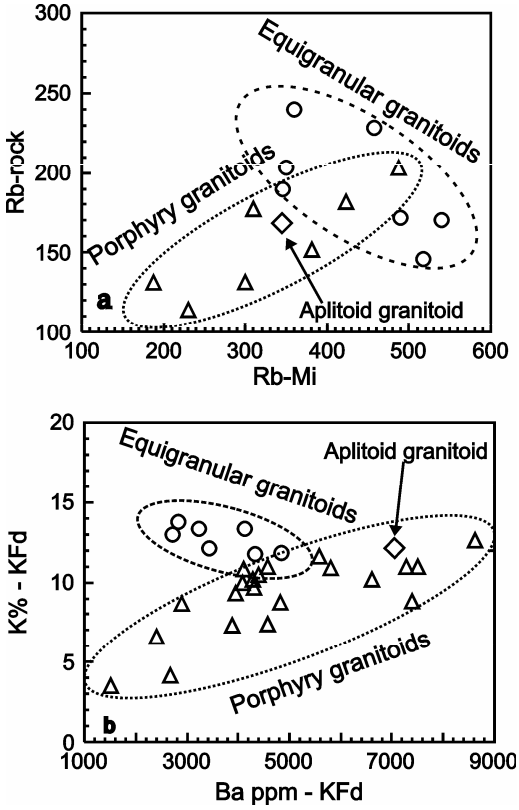

Fig. 4. Correlative relationships of some trace-elements in microclines: a) concentration of Rb in rock (Rb-rock) *vs.* concentration of Rb in microcline (Rb-Mi); b) concentration of K (%) *vs.* Ba (ppm) in K-feldspars

equigranular and positive for the porphyroid granitoids.

The contents of Ba in the potassium feldspars range 2300–7500 ppm. A tendency of increasing average quantities is outlined in the direction equigranular (3930 ppm, n=3) – porphyroid (4930 ppm, n=26) and probably to the aplitoid (7190 ppm, n=2) granitoids. Comparatively low are the Ba contents in the feldspars from pegmatites – 1179 ppm. Some granitoids from Rila and Rhodopes are quite similar – the average Ba content in their feldspars is 4440 ppm (n=41, Arnaudova & Arnaudov 1982). A similar tendency of increasing average contents of Sr in the potassium feldspars from equigranular (445 ppm, n=5) to porphyroid (474 ppm, n=26) and to aplitoid (544 ppm, n=2) granitoids is also noted. The microclines from the pegmatite veins and nests within the batholith are most depleted of Sr – the average content there is 289 ppm. Geochemical differences between the feldspars from the equigranular and porphyroid granitoids are shown on Fig. 4b, where the relationships between K and Ba in the microclines are compared. The correlation is negative for the equigranular and positive for the porphyroid granitoids.

The concentrations of Sr in microclines from Sakar batholith are approximately of the same order as in some granites of the so called "biotite-bearing facies" (Arnaudova & Arnaudov 1982) from Rila and Rhodopes (average 540 ppm, n=41) and from Sredna Gora (500 ppm, n=5).

Comparisons between the contents of trace elements in the cores and the rims of the microcline porphyries show that the rims are poorer in Sr, Ba, Rb, Li and Co, and richer in Th and U than the cores. This zoning is likely to be related to the higher albite component in the peripheral zones of the microclines and is indicative for the magmatic conditions of crystallization.

Biotite is the only femic rock-forming mineral in the rocks of the batholith. It is unevenly distributed in the rocks – around 5 vol.% in the central parts of the batholith and up to 22 vol.% in the western and southern marginal parts. The pleochroism scheme is ordinary dark-brown to dark-greenish-brown along the Z and Y axes. Biotites contain inclusions of apatite and zircon and are replaced by epidote and titanite. The more intensively altered biotites are full of chlorite with sagenite grid of acicular titanite crystals (Vergilov 1966). Around shear zones in the granitoids, the biotite flakes are grouped in indistinct strips and lenses or show planar orientation. In such cases biotites usually associate with secondary epidote, titanite and apatite.

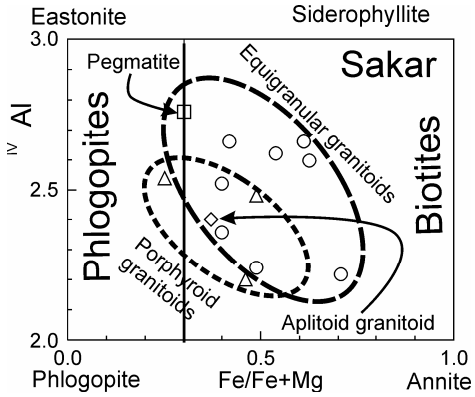

Fig. 5. Classification position of analyzed biotites from the batholith in a Fe/Fe+Mg *vs.* ^{IV}Al diagram

The chemically studied 13 samples of biotite are separated from artificial heavy rock concentrates (Fig. 5, Table 4). Almost all analyzed samples show lack of water in the site $(OH)_2$, which hints for the higher potential of oxygen in their magma. The absence of distinct changes in the parameters of the ferriferous, titanium and alumina contents of biotites from the different rock units indicates roughly constant and equal crystallization conditions. The combined phlogopite-eastonite and phlogopite-annite isomorphic replacement in the cell classify the biotites as ordinary varieties (Fig. 5) – the richer in Fe are the richer in ^{IV}Al. It seems that the biotites from the porphyroid and from the aplitoid granitoids have a little higher Mg and lower ^{IV}Al content than the biotites from the equigranular granitoids. The estimated oxidizing conditions of crystallization of biotites from Sakar batholith (Fig. 6) are higher than those from the biotites in Lessovo metagranitoids (Kamenov et al. 1986).

The agpaitic coefficient of the biotites is indicative for the alkalinity of their magmas (Marakushev & Tararin 1965). It determines also the progress of the eastonite isomorphic replacement (Mg, Fe)+Si → ^{VI}Al, ^{IV}Al. The average value of this coefficient for the equigranular rocks is 0.61 (range 0.56–0.71), whereas biotites from the porphyroid granites display higher and up to 0.69 (range 0.66–0.75) values. This supports the idea that there the crystallization of the large porphyroblastic microclines occurred at higher alkalinity conditions and had also an effect on the biotite composition. A comparison with biotites from Lessovo metagranitoids shows that the average value of this coefficient is lower (0.55) and hence, they should have been formed at lower alkalinity of their magma. According to the method of Marakushev & Tararin (1965) the biotites from the equigranular granitoids plot in the fields characteristic of normal and reduced alkalinity and those from the porphyroid granitoids – in the fields with moderately increased alkalinity. The application of the method of Abdel-Rahman (1994) refers biotites from the Sakar batholith to the calc-alkaline granites (Fig. 7). The relatively lower content of Al in biotites from the batholith in comparison with the biotite compositions in Lessovo orthometamorphic complex is typical for shallower depth of crystallization.

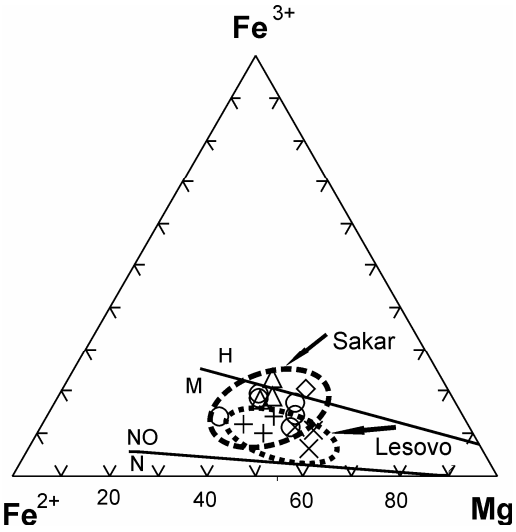

Fig. 6. Diagram Fe^{2+}-Fe^{3+}-Mg (after Wones & Eugster 1965) for biotites from the Sakar batholith and Lessovo orthometamorphites

Table 4. *Selected chemical composition of biotites and calculated formulae (based on 22 oxygens)*

Granitoids		Equigranular					Porphyroid			AGr
Sample		III/Bt	V/Bt	101/Bt	XIV/Bt	II/Bt	XIII/Bt	129/Bt	I/Bt	XVIII/Bt
Analysis		1	2	3	4	5	6	7	8	9
SiO_2		36.27	35.9	35.77	38.11	35.23	35.77	34.85	36.14	36.81
TiO_2		3.87	4.17	2.49	2.28	2.73	2.29	6.81	3.15	2.25
Al_2O_3		15.15	14.6	16.47	17.13	15.03	17.54	11.91	14.33	17.54
Fe_2O_3		6.2	7.1	4.75	7.63	7.66	6.86	7.99	7.46	8.47
FeO		13.21	12.4	13.99	13.87	15.07	12.96	14.21	15.11	10.74
MnO		0.32	0.43	0.34	0.68	0.55	0.48	0.46	0.45	0.46
MgO		11.01	1039	10.96	8.03	8.8	10.63	9.56	9	10.21
CaO		0.42	1.91	1.77	1.46	0.56	1.08	2.67	1.5	1.43
Na_2O		0.1	0.12	0.25	0.66	0.15	0.01	0.2	0.35	0.56
K_2O		10.42	8.88	8.11	6.86	3.74	8.67	7.57	8.96	8.55
P_2O_5		0.12	0.2	0.41	0.08	0.13	0.09	0.35	-	0.1
H_2O^-		0.3	0.27	0.4	0.41	0.45	0.47	0.84	0.34	0.24
H_2O^+		2.23	3.54	4.73	2.96	4.41	3.15	2.93	3.69	2.52
Total		99.62	99.8	100.4	100.16	100.5	99.99	100.4	100.5	99.88
Cs		6.2	49.1	-	28	26.5	16.2	17.8	20.1	14.6
Ba		362	238	-	430	381	455	505	473	408
Rb		429	988	-	650	605	456	590	474	420
Cr		63	77	-	55	30	55	66	50	56
V		354	-	-	112	-	273	-	-	274
Th		2.3	20	-	16.7	12.2	3.9	10	15.8	5.3
U		0.2	6.5	-	3.6	5	-	-	3.1	-
Hf		1	5.8	-	5.6	4.1	1	13	4.2	1.6
Ta		-	13.8	-	2	1.1	0.8	5.2	2.7	0.4
Sc		7.2	11.2	-	9	6.8	8.8	16.2	10.1	8.7
Zn		241	449	-	704	474	204	318	232	201
Co		34	42	-	31	23	29.3	33.7	26	28.4
	K	2.08	1.72	1.54	1.32	1.9	1.68	1.5	1.74	1.66
	Na	0.02	0.04	0.08	0.18	0.04	-	0.06	0.1	0.16
	Ca	-	0.24	0.2	0.22	0.06	0.16	0.36	0.16	0.18
X		2.1	2	1.82	1.72	2	1.84	1.92	2	2
	Ca	0.04	0.01	-	-	-	-	-	0.08	0.04
	Mg	2.54	2.36	2.44	1.8	2	2.4	2.22	2.04	2.32
	Fe^{2+}	1.72	1.58	1.74	1.74	1.92	0.78	1.86	1.92	1.36
	Fe^{3+}	0.72	0.82	0.54	0.86	0.88	1.64	0.94	0.86	0.96
	Mn	0.04	0.06	0.04	0.08	0.06	0.06	0.06	0.06	0.06
	Ti	0.46	0.48	0.28	0.26	0.32	0.26	0.44	0.36	0.26
	Al	0.42	0.1	0.24	0.8	0.08	0.58	-	0.1	0.74
Y		5.94	5.41	5.28	5.54	5.26	5.72	5.52	5.42	5.74
	Si	5.64	5.48	5.34	5.76	5.38	5.44	5.8	5.52	5.6
	Al	2.36	2.52	2.66	2.24	2.62	2.56	2.2	2.48	2.4
O_{20}	O	20	20	19.28	20	19.52	20	20	20	20
	OH	-	-	0.72	-	0.48	-	-	-	-
$(OH)_2$	O	1.68	0.4	0	1.02	-	0.8	0.94	0.24	1.44
	OH	2.32	3.6	4	2.98	4	3.2	3.06	3.76	2.56
$Mg^{\#}$		0.6	0.6	0.58	0.51	0.51	0.75	0.54	0.51	0.63
Fe^{3+}/Fe^{2+}		0.42	0.52	0.31	0.49	0.46	2.1	0.5	0.45	0.7

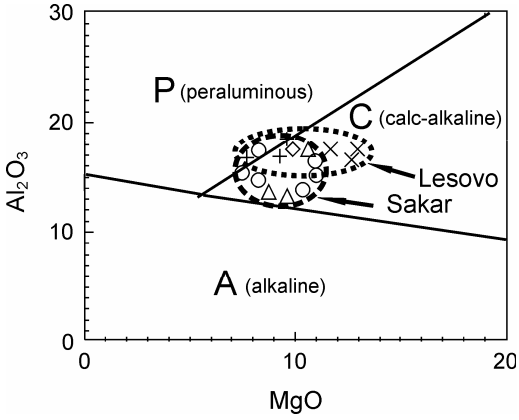

Fig. 7. Discrimination plot MgO *vs.* Al_2O_3 after Abdel-Rahman (1994) for biotites with fields for the Sakar batholith and Lessovo orthometamorphites

Compared to the biotites from other complexes using Al_2O_3 contents, biotites from Sakar batholith are similar to the biotites from Rila-Rhodopes and Sredna Gora granites, but with their higher contents of TiO_2 they are closer to the Osogovo and Pirin granitoids (Arnaudova & Arnaudov 1982).

Muscovite. Two types of muscovite are distinguished. The coarse-flaked (up to 1.5 mm) variety with fully developed faces and co-existing with the biotite is more common in the peraluminous granites. The analyzed two mon-omineral samples of this type (Table 5) plot on the discrimination Mg-Fe-Ti (Speer 1984; Monier et al. 1984) clearly in the field of the muscovite of magmatic origin. In some places muscovite flakes are grouped into parallel strips and obviously are deformed. The fine-flaked muscovite is developed mainly over the coarse-grained plagioclases and associates often with epidote and clinozoizite, less commonly with calcite. It is a secondary by origin result of the autometasomatic influence of late solutions on the granite, but could be also a sign of regressive metamorphism around the zones of deformation or close to shear zones.

Quartz in the equigranular and in the porphyroid varieties usually forms irregular

Table 5. *Chemical composition and calculated formulae of selected muscovites from equigranular granitoids*

Sample		VI/Ms	XII/Ms
SiO_2		46.99	46.64
TiO_2		1.22	1.18
Al_2O_3		28.51	26.27
Fe_2O_3		5.28	5.14
FeO		1.46	1.82
MnO		0.07	0.11
MgO		1.79	2.28
CaO		0.75	1.09
Na_2O		0.40	tr.
K_2O		7.67	10.14
P_2O_5		0.45	0.07
H_2O^-		0.20	0.36
H_2O^+		4.83	4.84
Total		99.62	99.94
Li		95	140
Rb		617	501
Ba		772	476
Th		21.0	19.8
U		7.9	6.6
W		9.0	4.9
Hf		1.5	5.3
Ta		6.0	5.1
Cr		14	18
Sc		16.0	26.6
ΣCe/ΣY		20.9	59.8
Th/U		2.7	3.0
Cu		-	7
Zn		207	184
Calculated formulae-10 O			
	K	0.66	0.88
	Na	0.05	0
	Ca	0.01	0.07
X		0.72	0.95
	Mg	0.18	0.23
	Fe^{2+}	0.08	0.10
	Fe^{3+}	0.27	0.26
	Mn	0.004	0.006
	Ti	0.06	0.06
	Al	1.44	1.29
Y		2.03	1.96
	Si	3.17	3.18
	Al	0.83	0.82
Z		4.00	4.00
	O	9.93	9.80
	OH	0.17	0.20
O_{10}		10.00	10.00
	$(OH)_2$	2.00	2.00

Sample VI/Ms contains 1.08 % apatite and sample XII/Ms – 0.84 % apatite

Table 6. *Chemical composition of selected representative samples from Sakar batholith*

Granitoids	Equigranular					Porphyroid			
Sample	137/S	121/S	II/S	VI/S	XII/S	IV/S	101	119	141
Rock	Qmz	Gd	Gr	Gr	Slg	Mz	Qsy	Gr	Gr
SiO_2	61.80	64.47	71.35	72.45	73.31	62.14	64.23	66.60	68.57
TiO_2	0.46	0.80	0.34	0.24	0.14	0.85	0.60	0.47	0.48
Al_2O_3	17.89	15.33	14.12	14.12	13.52	16.45	14.47	15.78	14.36
Fe_2O_3	3.07	3.12	0.70	0.84	0.68	1.74	2.12	2.55	1.84
FeO	1.70	1.90	1.33	0.85	0.55	2.59	1.98	0.99	0.84
MnO	0.09	0.07	0.04	0.03	0.03	0.09	0.12	0.06	0.09
MgO	1.61	2.10	0.74	0.78	0.40	2.60	2.15	1.39	1.27
CaO	3.98	3.62	2.26	1.82	1.77	3.79	3.72	2.77	2.75
Na_2O	4.60	4.30	3.96	3.79	3.27	3.99	4.30	4.46	3.53
K_2O	3.40	3.20	4.13	4.41	5.15	4.48	4.32	3.82	4.26
P_2O_5	0.37	0.30	0.11	0.15	-	0.35	0.28	0.22	0.23
H_2O^-	0.18	0.10	0.04	0.05	0.11	0.12	0.13	0.08	-
H_2O^+	1.13	0.82	0.52	0.71	0.57	0.52	1.71	1.01	1.41
SO_3	0.07	0.12	0.07	0.09	-	0.09	0.19	0.10	0.11
Total	100.35	100.25	99.71	100.33	99.50	99.81	100.32	100.30	99.74
An%	37	26	20	20	20	29	17	24	26
Li	15	20	20	10	24	10	15	20	30
Cs	5.7	3.0	5	3	2.2	2	3.5	3.7	1.5
Th	13.6	12.7	9.3	10.1	8.6	10.8	4.6	17.4	9.6
U	9.4	3.7	6.5	3.3	4.1	4.0	2.9	5.4	5.8
La	31.4	38.3	25	30	21.3	25	48.2	31	24.2
Ce	55	61	37	46	31.5	40	72	53	40
Sm	5.8	6.0	4.4	4.9	4.4	4.0	7.6	4.9	4.8
Eu	1.06	0.97	0.55	0.82	0.5	0.30	0.85	0.51	0.63
Tb	1.0	1.1	0.7	0.85	0.5	0.6	1.5	0.8	0.8
Yb	1.2	2.4	1.6	1.9	0.9	1.2	2.6	1.6	2.1
Lu	0.44	0.53	0.34	0.40	0.34	0.31	0.51	0.38	0.50
Ba	724	618	424	537	1259	984	1009	306	649
Sr	415	381	268	311	305	362	328	284	237
Zr	210	143	111	124	75	185	195	137	146
Rb	133	225	190	215	240	165	199	182	156
Hf	6.0	4.5	3.2	3.7	2.4	2.5	5.2	3.1	3.4
Ta	3.0	1.3	0.9	1.0	0.9	0.9	2.7	1.0	1.7
Cr	13	18	14	60	10	4.0	-	6.0	6.0
Sc	6.3	6.0	5.0	110.0	1.4	2.0	7.0	3.3	5.0
V	115	133	38	32	<20	122	76	73	70
Zn	41	61	44	37	23	18	220		42
Ni	3	4	-	13	12	-	2	1	-
Au	0.001	0.0014	0.009	0.006	0.009	0.0066	-	0.0075	0.0016

nest-like or even strip-like coarse-grained aggregates. It contains abundant inclusions of difficult to diagnose acicular mineral, probably rutile and very rare fine-grained biotite flakes, zircon and epidote crystals. The fine-grained quartz crystals are quite pure of inclusions. Within the aplitoid granites quartz is anhedral and forms isometric crystals, containing only some evenly distributed dust-like inclusions.

Accessories are titanite, apatite, zircon and allanite. The aplitoid granites contain also garnet. Titanite is particularly common, being

best developed in the porphyroid granitoids. Allanite forms elongated along the crystallographic axis *b* up to 0.5 mm large crystals, all overgrown epitaxially with epidote envelopes. Metamict altered crystals are also met. The magmatic origin of allanite is supported by it strong zonation.

Petrochemistry

Statistical parameters of the oxide distributions are shown in Table 7. The correlation coefficients between the oxides are investigated separately for each rock unit. One of the substantial differences between the equigranular and porphyroid units is the number of significant correlations, which is higher in the first unit (7), while no one of these correlations is preserved in the porphyroid granitoids. The implication is that these correlations are typical for the magmatic crystallization. For instance, SiO_2 in the equigranular granitoids correlates highly positive with K_2O and weakly negative – with Na_2O, whereas in the porphyroid granitoids there is no correlation between K_2O and SiO_2, but such a correlation exists between SiO_2 and Na_2O. The secondary re-distribution of Na_2O, related to the superimposed albitization, disturbed the magmatic correlation, but did not affect the correlation between K_2O and SiO_2. On the contrary, the superimposed redistribution of K_2O (on account of the late-magmatic porphyroblastesis) in the porphyroid granitoids influenced all significant correlations, provoked by the magmatic crystallization, and obliterated them. If we disregard the modified correlative relationships, both rock units do not differ essentially in their other statistical parameters of the major oxides.

Most of the rock samples are metaluminous and a small part of them are peraluminous (Fig. 8). The juxtaposing of the normative colour index with the normative anorthite composition of the plagioclases (Fig. 9) does not reveal important differences between the equigranular and the porphyroid granitoids, but the aplitoid granites are distinguished with their poorness of femic

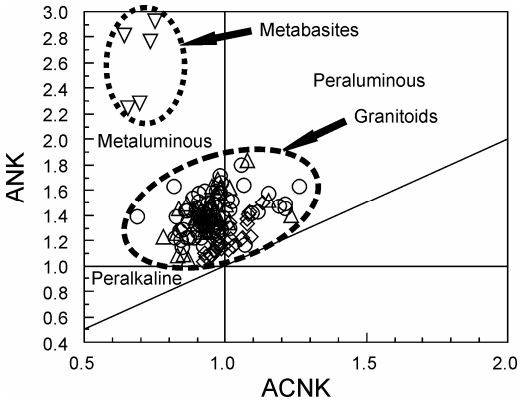

Fig. 8. A/CNK *vs.* A/NK diagram for samples from the Sakar batholith

components and their more acid plagioclases. Harker's diagrammes (Fig. 10) illustrate the most important distributions of the major oxides in the rocks. The negative correlations between SiO_2 and TiO_2, Al_2O_3, FeO, MnO, MgO, CaO and P_2O_5 are characteristic for a common magmatic evolution of a calc-alkaline serial type caused by fractionation of femic minerals and plagioclase. The petrochemical evolution is well seen on the TAS diagram in Fig. 11 (Efremova & Stafeev 1985) where the

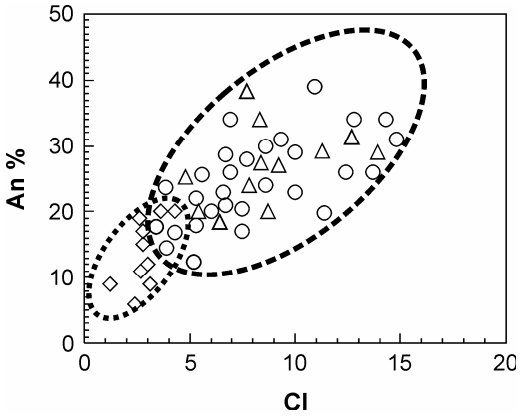

Fig. 9. Variation diagram color index (CI) *vs.* normative anorthite composition (An %) for rocks from the batholith

Table 7. *Statistical parametres for the wt.% major oxides and ppm trace elements of the rocks from the batholith*

Granitoids	Equigranular			Porphyroid			Aplitoid		
Parameter	X	S	V %	X	S	V %	X	S	V %
Number	n=63			n=37			n=25		
SiO_2	68.16	3.45	5	68.14	0.49	14.93	73.68	1.49	2
TiO_2	0.49	0.27	1.2	0.49	0.13	26	0.12	0.09	7
Al_2O_3	15.4	1.23	8	14.93	0.83	6	13.82	0.78	6
Fe_2O_3	1.30	1.19	91	1.56	0.77	50	0.61	0.35	58
FeO	1.56	0.86	55	1.56	0.95	61	0.38	0.25	66
MnO	0.06	0.03	48	0.08	0.03	37	0.03	0.02	94
MgO	1.20	0.57	47	1.31	0.58	44	0.44	0.22	51
CaO	2.85	1.02	36	2.87	0.73	26	1.20	0.35	29
Na_2O	4.09	1.08	26	4.03	0.54	13	3.71	0.68	18
K_2O	3.87	1.04	27	3.76	0.17	15	5.01	1.28	26
P_2O_5	0.18	0.08	43	0.19	0.07	37	0.14	0.07	48
H_2O^+	0.35	0.39	112	0.59	0.49	82	0.32	0.34	11
Number	n=33			n=33			n=17		
Rb	155	39	26	156	37	24	175	50	28
Li	24	10	43	22	8	39	12	3.5	28
Cs	3.4	1.5	47	3.0	1.3	38	2.5	1.2	78
Ba	787	212	27	684	222	38	335	294	88
Sr	355	88	25	309	62	20	125	64	49
Zr	144	29	20	150	26	18	60	33	55
La	32.6	8.8	27	34.7	14	41	8.1	10	129
Ce	52.7	15.7	30	56.2	23	41	12	9	74
Sm	5.1	1.6	32	5.7	2	30	2.6	2.8	107
Eu	0.7	0.3	37	0.8	0.4	47	0.19	0.1	51
Tb	0.8	0.2	30	0.9	0.4	41	0.59	0.6	96
Yb	1.5	0.5	31	1.8	0.8	43	1.8	1.5	84
Lu	0.4	0.1	37	0.4	0.1	32	0.37	0.5	149
Th	16.3	7.6	47	12.6	6	43	6.8	8.1	118
U	5.1	2.1	42	4.8	2	35	5.1	8.6	168
Hf	3.6	0.9	27	3.8	1.1	29	1.9	1.6	84
Ta	1.3	0.5	40	1.7	1	48	2.9	2.6	88
Cr	24	26	108	19	16	84	5.6	3.3	60
Sc	4.5	2.5	56	4.7	1.6	34	1.7	0.5	30
As	1.1	0.5	50	1.2	1	66	1.3	0.4	34
Sb	0.17	0.1	60	0.18	0.12	64	0.14	0.08	57
Zn	53	18	35	58	39	68	46	15	32
Mo	8.7	4.1	47	7.2	4.8	66	4.2	3.2	75
Ni	18	14	75	14	13	96	6.2	3.7	60
Co	5.2	3.1	60	4.8	2	22	0.96	0.5	55
V	53	33	62	59	22	37	16	4.9	30
Au	0.004	0.003	78	0.003	0.002	70	0.003	0.002	57
K/Rb	230	54	23	204	40	19	258	75	29
Th/U	3.5	1.4	40	2.5	0.73	29	2.0	1.2	61

fields of the equigranular and porphyroid granitoids almost fully overlap. The total alkalies range is too wide, which is indicative for their mobility due to the influence of postmagmatic re-distribution.

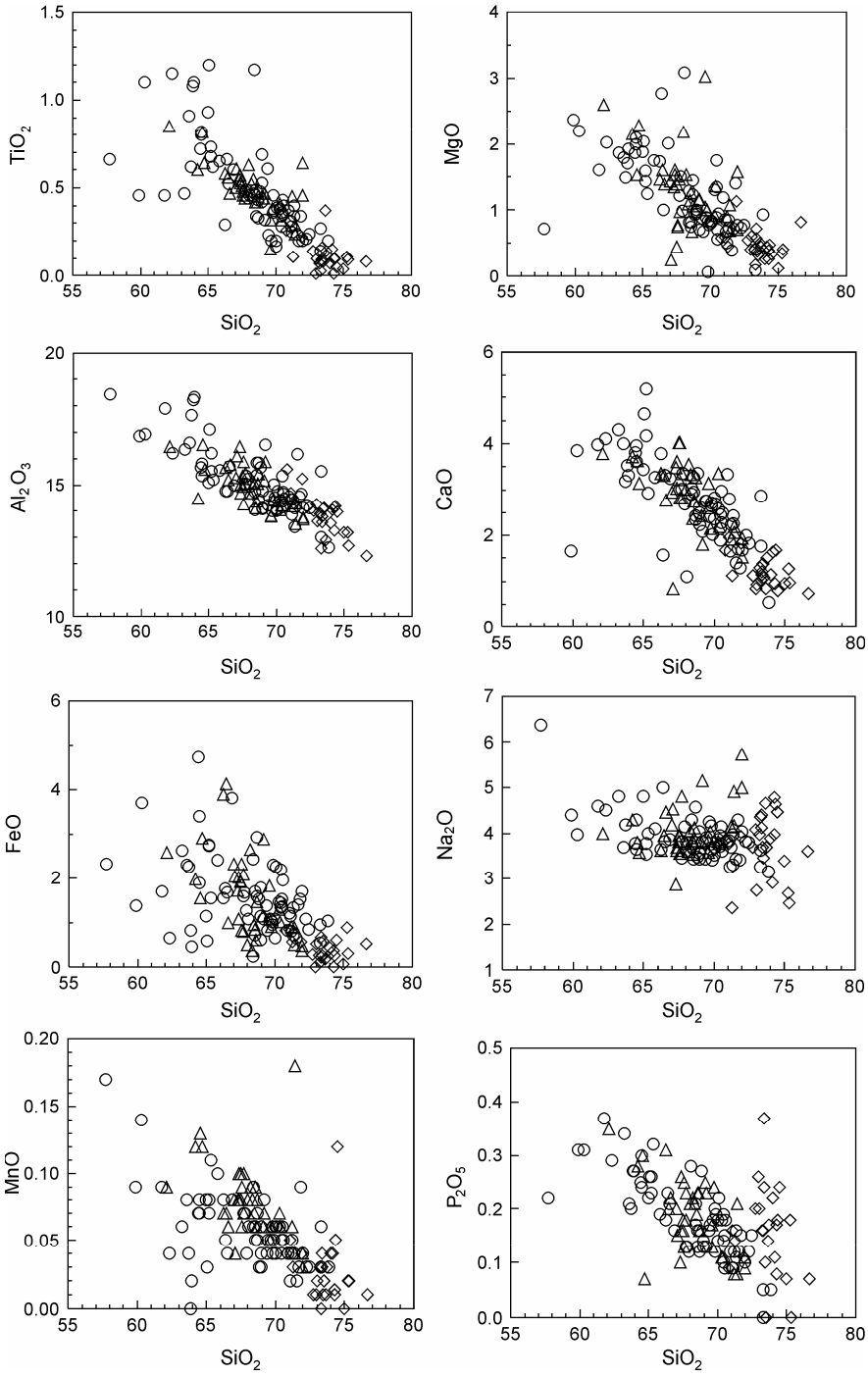

Fig. 10. Selected Harker diagrams for the major oxides in rocks from the Sakar batholith

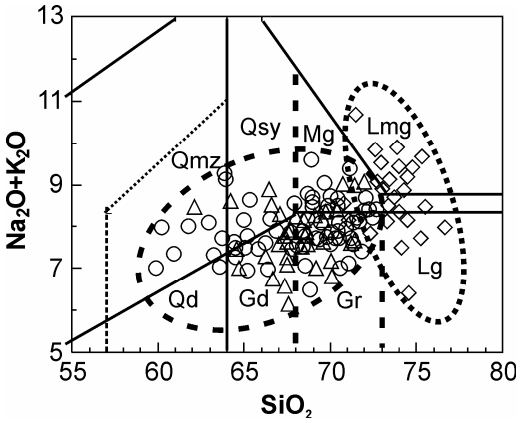

Fig. 11. TAS diagram (after Efremova & Stafeev 1985) for samples from the batholith

The principal part of the analyzed samples falls in the high-potassium calc-alkaline series on the K_2O *vs.* SiO_2 diagram (Fig. 12). The deviations to the calc-alkaline and the shoshonite series are comparatively few. Only the concentrations of K_2O in the aplitoid granitoids are too dispersed and they fall into several series. The probable reason is the stronger fluid impact on their magmas.

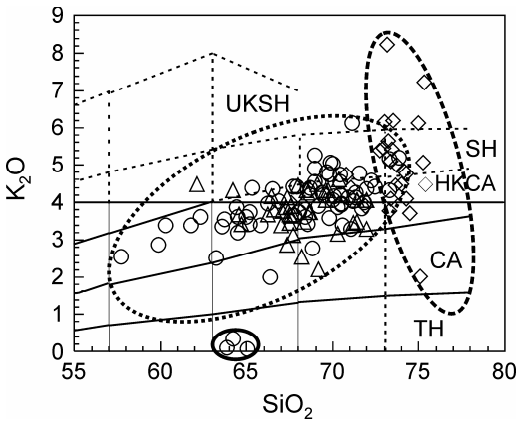

Fig. 12. SiO_2 *vs.* K_2O plot (Peccerillo & Taylor 1976) extended (hatched lines) by Dabovski et al. (1989). Points in solid ellipse: albitized granites

Eventually, the depletion of K_2O in the more acid rocks of the porphyroid unit and the obvious lack of positive correlation between K_2O and SiO_2 are due to re-crystallization connected with the porphyry formation in the endocontact parts of the pluton, in spite of the fact that the average chemical compositions of the equigranular and porphyroid units almost coincide.

The spatial distribution of K_2O contents within the rocks of the batholith is shown in Fig. 13. The lines of equal K_2O contents portray typical zoning, revealing the dome-like structure of the batholith in another way. This zoning is not only horizontal, but also vertical since the highest hypsometric levels in Sakar Mountain coincide with the central parts of the batholith, so that the rocks there are richer in K_2O. The exposures of the aplitoid granites were not considered when the map was compiled because of their small outcrops.

Geochemical differences between the rock units are sought by analysis of the correlation between the ratio K_2O/MgO and SiO_2 (Fig.14). K_2O is selected as one of the most incompatible components, while MgO is the oxide with the strongest compatible behaviour in the course of the crystallization, SiO_2 content being also a measure for its progress. The positive correlation visualizes well the chemical changes in the magma evolution, but here the porphyroid granitoids are also in the outlines of a common field with the samples from the equaligranular granitoids and no whatever correlation is expressed. The intensively albitized rocks of the equigranular granitoids are outlined distinctly with their lower ratios K_2O/MgO. Similar relationships are shown in this figure for the xenoliths of orthoamphibolites in the batholith.

Geochemistry

Analysis of the Clarke's of concentration in the rock samples leads to the following conclusions: (1) the elements U, Hf, Sc, Mo, Ni, V and W have over clarkes concentrations in the rocks. It is most likely that the contamination

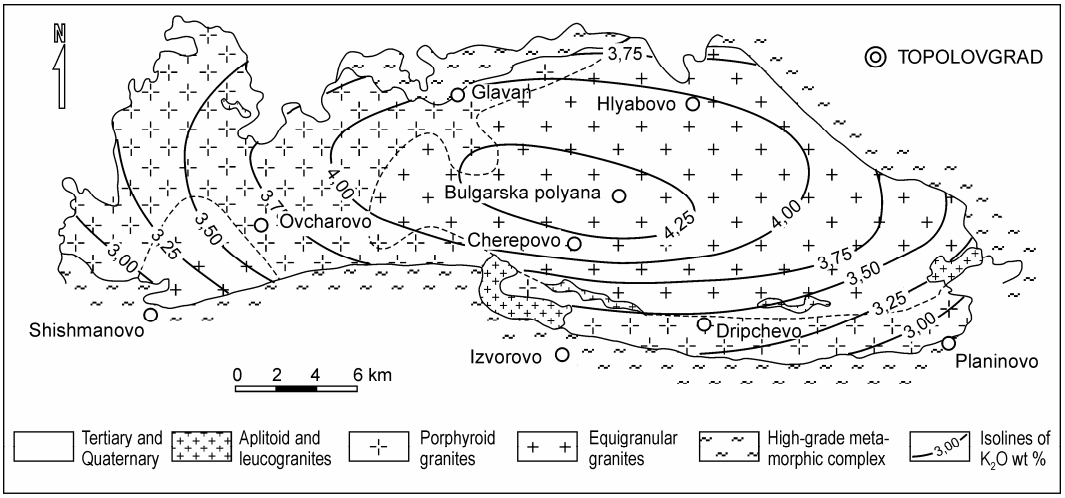

Fig. 13. Sketch map of Sakar batholith with lines of equal contents of K_2O in the equigranular and porphyroid granitoids

left traces in the relative richness of biotite and this is the reason for the overclarkes concentrations of the elements Hf, Sc, V and Ni; (2) Nearly around the clarkes is the amount of Sr, Ba, Th, Zn, Co, Cr and Au; (3) Below the clarkes are the trace elements Rb, Li, Cs, Zr, *REE*, Ta, As, and Sb; (4) The compatible elements with consecutively decreasing clarkes of concentration are P, Cr, Sc, V, Co, Ni, and Mo. These components are related to the fractionation of biotite and apatite. Examples of this geochemical association are shown in Fig. 15. The same association of elements includes also Li, Ba, Sr, Zr, U and Th, which is depleted predominantly in the aplitoid granites on account of their combining in the earlier crystallized equigranular and porphyroid granitoids. One of the reasons for this behaviour is the plagioclase fractionation in the earlier magmas; (5) The elements with consecutively increasing clarkes of concentration and having clear incompatible behaviour are K, Rb and Ta. (6) A group of trace-elements shows maxima in the porphyroid granitoids, but the last aplitoid phases are strongly depleted in Cs, *REE*, Hf, Zn, As, and Au. The preferable mobilization of alkalies during the process of the endoblastic porphyry growth influenced the re-distributions of Cs and U and the superimposed later hydrothermal impact introduced Zn, As and Au. It seems that in the course of re-crystallization and growth of microcline porphyroids, the infiltration fluxes have exported U together with K.

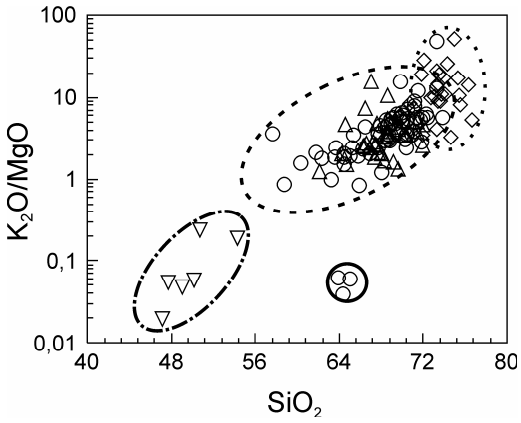

Fig. 14. SiO_2 *vs.* K_2O/MgO plot for rocks from the batholith. Dash-dotted ellipse: samples from ortho-amphibolites

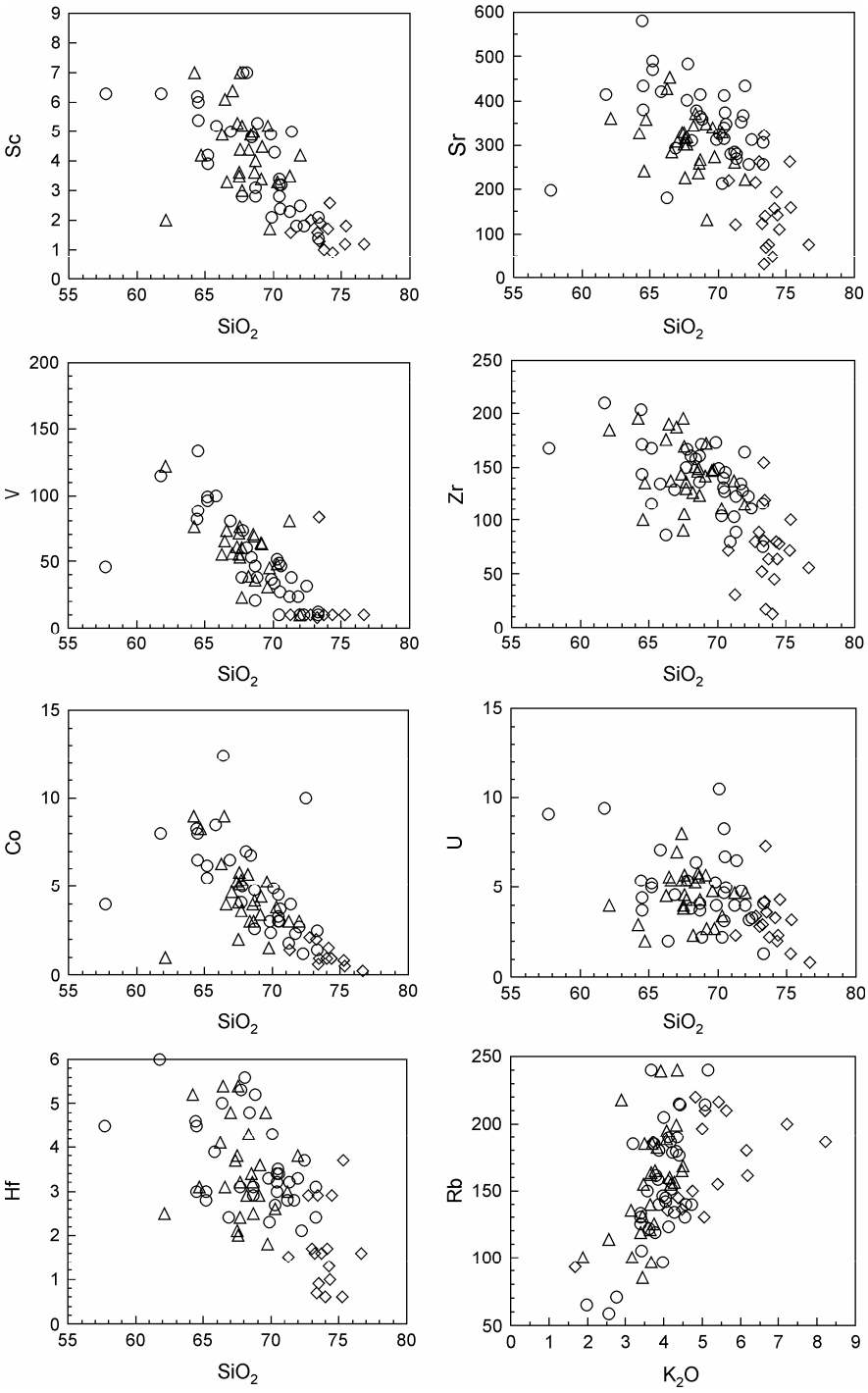

Fig. 15. Selected Harker diagrams for the trace-elements in rocks of the batholith

The strong geochemical correlation between K and Rb is demonstrated on the last plot in Fig. 15. The fairly stronger correlation for the granitoids showing lower Rb concentrations is typical for the processes of crystallization differentiation. The diminution of the correlation at higher concentrations reflects the superimposed re-crystallization in the porphyroid granitoids and the stronger fluid input in the aplitoid remnants.

Plagioclase is the main mineral-carrier and concentrator of Sr in the rocks. Regardless of the fact that the average Sr contents decrease in the rock units from the equigranular to the porphyroid granitoids (Table 7), the differences between these two units are not significant, but the aplitoid granites differ distinctly by their too low Sr concentrations. The ratio Rb/Sr in these leucogranite rock varieties is much higher, in spite of its wide range (Fig. 16). The main reason for these differences is the fractionation of the feldspars as the plotted vectors (Harris et al. 1986) suggest, while the width of the common field for the equigranular and the porphyroid granitoids may depend on the degree of biotite fractionation.

Plagioclase, biotite and microcline are minerals-carriers of Ba, but the last mineral is the main mineral-concentrator of this element.

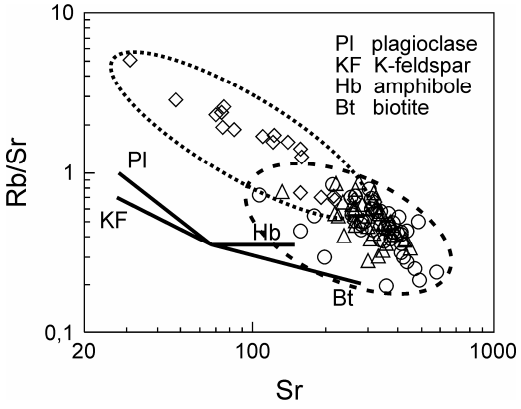

Fig. 16. Sr *vs.* Rb/Sr plot for samples from the batholith. Fractionation vectors are after Harris et al. (1986)

The ratios Ba/Sr and Ba/Zr are variable and quite similar in the equigranular and porphyroid granitoids, but they are considerably higher in the aplitoid granites. At a relatively equal level of Ba concentrations in the rocks, the lower Sr and Zr concentrations in the aplitoid granites are responsible for this specific feature. The metabasic xenoliths in the batholith are clearly distinguished by their lowest Ba contents.

The Th concentrations in the rocks are approximately of the same order (Table 7), but if only their average values are considered, they are decreasing similarly to the U concentrations. The roughly equal range of the ratios Th/U in all rock units emphasizes their co-genetic character. It seems that only the aplitoid granites are richer in U, which was probably hydrothermally/fluid imported in the remnants of the magmatic evolution.

Rare earth elements (*REE*) in the rocks and minerals (Tables 1, 2, 3, 4, 5, and 6) are studied in the chondrite-normalized patterns (Figs. 17, 18). All samples display negative Eu-anomaly. If the ratio $(Eu/Sm)_N$ is used as a measure of this anomaly, then there is no statistically meaningful difference between the equigranular (average Eu_N/Sm_N=0.13) and the porphyroid granitoids (average Eu_N/Sm_N=0.14), but the depth of this anomaly is essentially larger in the aplitoid granites (average Eu_N/Sm_N=0.08). In the granitoids of increased alkalinity in the first two units (quartz-monzonite, monzogranite, and quartz-syenite, Figs. 16b, d) the Eu-anomaly is stronger, which is related to the increased proportions of plagioclase fractionation in these rock units. The negative Eu-anomaly in the rock varieties with normal calc-alkaline characteristic (granodiorite and granite – Figs. 17a, c) is relatively shallower. The degree of enrichment of *LREE* relative to *HREE* and the total sum of *REE* refer the rocks from the batholith to the group of granitoids with typical for the marginal continental settings geochemical affinity (Cullers & Graff 1984). The average ratios $(La/Lu)_N$ between the equigranular (8.5) and porphyroid granitoids

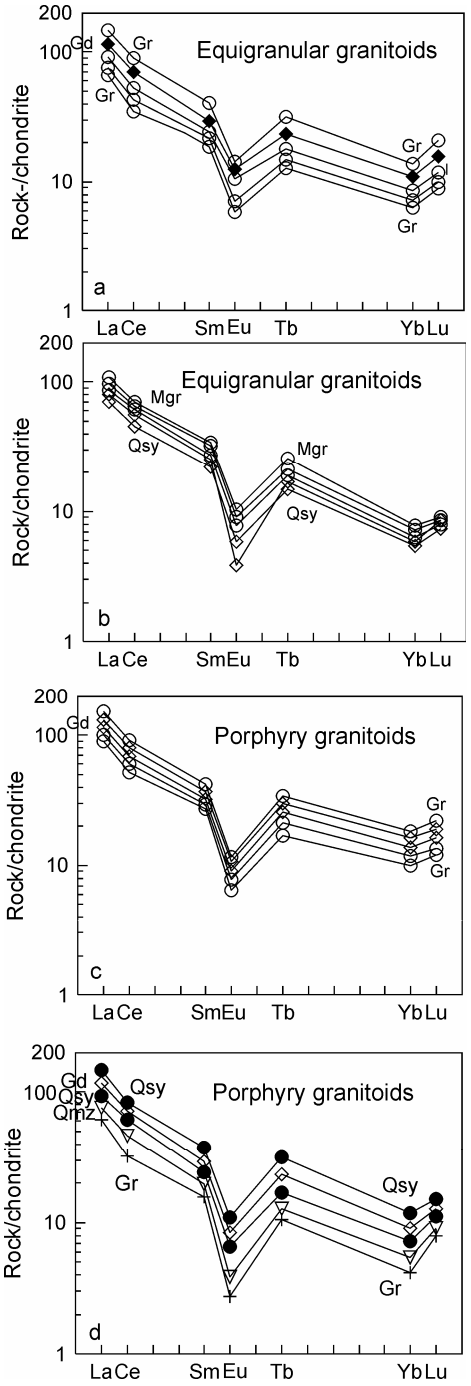

Fig. 17. Chondrite-normalized *REE* patterns for samples from the batholith

(9.0) are again similar, but the slope of the normalized curves in the aplitoid granitoids $(La/Lu)_N$=2.3) is much smaller or missing at all and the total sum of *REE* is also lower. Analyzing the features of the normalized *REE* patterns in the aplitoid granites (Figs. 18a, b) we could distinguish additionally two subassociations: (1) of the typical aplitoid leucogranites, characterized with the depleted pattern similar to that of the aplites and bearing to their residuum character and (2) of the transitional in alkalinity leucogranites with more fractionated *LREE*.

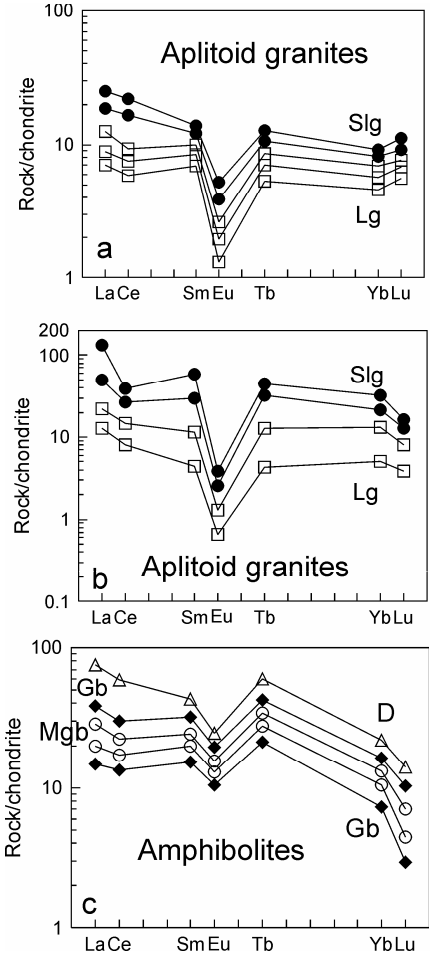

Fig. 18. Chondrite-normalized *REE* patterns for samples from the batholiths

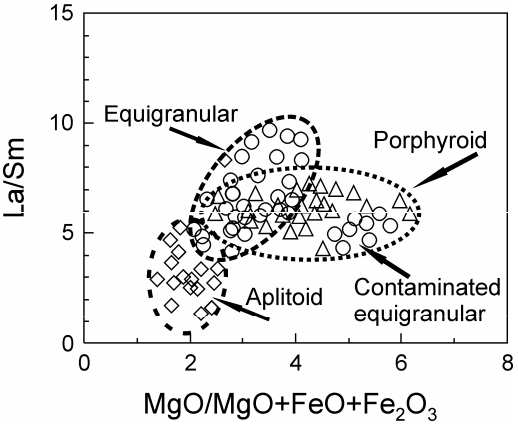

Fig. 19. $MgO/MgO+FeO+Fe_2O_3$ *vs.* La/Sm plot for samples from the batholith

The enrichment degree of *LREE* is studied on a diagramme La/Sm *vs*. $MgO/MgO+FeO+Fe_2O_3$ (an analogy to the melanocratic features of the rocks). The systematic decrease of *REE* enrichment in the sequence equaligranular–porphyroid–aplitoid granitoids (Fig. 19) is violated just in the porphyroid unit, where no correlation is practically found. The re-distribution of components during the course of the late-magmatic porphyry formation disturbed the correlation so that the leucocratic-melanocratic variations did not lead to changes in the La/Sm ratio. An interesting fact is that the field of the porphyroid granitoids includes a detached group of samples of equaligranular granitoids, which turned out to be melanocratic varieties sampled around the amphibolite xenoliths, hence influenced by contamination.

Except for the strong correlations between the elements inside the group of *REE*, which is a well-known geochemical feature, some positive correlations of La and Ce with Th, Hf and As are characteristic for the equigranular granitoids. Unusual positive correlations are expressed in the porphyroid granitoids of *LREE* with the typically femaphile elements like Cr, Sc, Zn, Ni and Co and also of *HREE* with U. The obliteration of the primary magmatic correlations and the appearance of new correlations is a consequence of the process of endocontact re-distributions related to the microcline porphyry formation. Almost all *REE* are positive correlated significantly with As in the aplitoid granites and in the combination of strong correlations of *LREE* is included also U.

Nearly all rocks in the batholith show positive Lu-anomaly, which is difficult to explain for the time being, not excluding systematic analytical errors.

The separately analyzed cores and rims of K-feldspar porphyries reveal that the rims are richer in *LREE* and poorer in *HREE*. The interpretation is that at the end of the processes of endocontact re-crystallization, related to the porphyry formation, the *REE* geochemical specialization fixed higher amount of *REE* in agreement with the higher alkalies potential. Obviously, the differentiated behaviour of the incompatible mobile elements in the marginal zones of the batholith applies to *REE* as well.

Some distinctions of the *REE* contents in the different granitoid varieties become apparent when their potassium feldspars are analyzed. The microclines from the equigranular granitoids are characterized by lower total *REE* sum, a bit weaker degree of *LREE* enrichment and more strongly expressed positive Eu-anomalies, as compared to the microclines from the porphyroid granitoids (Fig. 20a). The lowest *REE* sum is established in the microclines from the aplitoid granites. Similar regularities are revealed for the *REE* distributions in the biotites from different rock units. The analyzed biotites from the equigranular granitoids are stronger enriched in *LREE* and at the same time in *HREE*, compared to the biotites from the porphyroid granitoids and they display deeper negative Eu-anomalies. Except for the shallower Eu-anomalies, the chondrite-normalized patterns of biotites from the porphyroid granitoids are more often disturbed and irregular. A possible explanation is that perhaps some restitic biotites from the xenoliths after their granitization were preserved and left traces in their *REE* models.

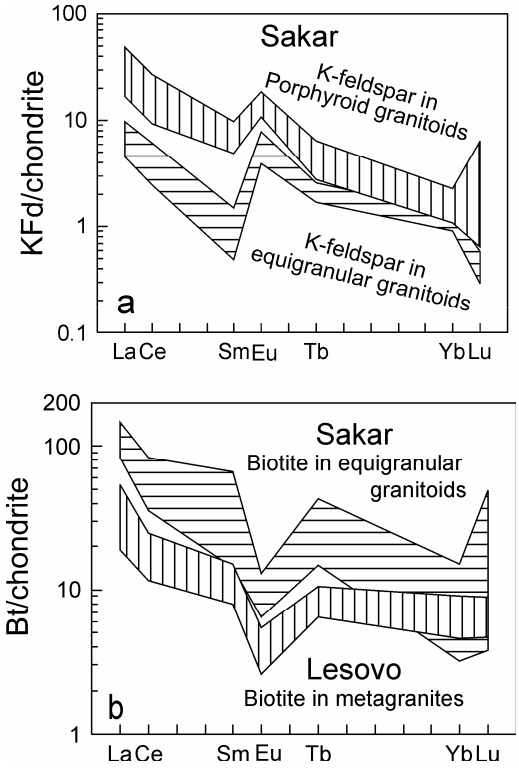

Fig. 20. Chondrite-normalized *REE* patterns for rock-forming minerals

Another interpretation implicates some post-magmatic re-equilibration as responsible for this specific feature.

The *REE*-patterns of biotites from Lessovo orthometamorphic complex have not only lower total *REE* sums, but they are also closer to the patterns of biotites from the porphyroid granitoids in Sakar batholith (Fig. 20b). This similarity supports the speculation that possibly biotite "ghost shadows" may be preserved in the around-contact parts of the batholith, where Lessovo type metagranitoids are country rocks.

A comparison between the *REE* normalized contents in the rocks and the *REE* patterns of the major rock-forming minerals (Tables 1, 2, 3, 4 and 5) leads to the following conclusions: (1) The amounts of *REE* in the rocks are unbalanced with respect to their individual contents in the rock-forming minerals (potassium feldspar, plagioclase, biotite and muscovite). Our assumption is that the shortage of *REE* was related to the accessories, which were not analyzed due to technical problems in their separation. The most likely mineral-concentrators of *REE* in the rocks of the batholith are epidote, allanite, clinozoizite, apatite, titanite and zircon. The high quantity of epidote minerals inevitably would contribute to the negative Eu-anomalies and to *LREE* enrichments in the rocks. (2) The appearance of muscovite in the granitoids increases the *LREE* enrichment in the rock patterns; apatite also contributes to this feature. (3) The main mineral-carriers of *REE* in the rocks are biotite and plagioclase and also muscovite in some cases. The bulk distribution coefficient of *REE* concentration in biotite to the one in the rock is $D^{REE}>1$. The main mineral-carrier of *LREE* in the two-mica rock varieties is muscovite, while biotite is a carrier of *HREE*. (4) The increased proportion of biotite in some of the rocks from the batholith may be also a reason for the positive Lu-anomaly in the patterns. (5) The essential rock-forming minerals constitute the following sequence of decreasing contribution of *REE* to the rocks: biotite–muscovite–plagioclase–potassium feldspar. All essential rock-forming minerals in the porphyroid granitoids have most often a negative distribution coefficient of their *REE* (concentration of *REE* in the mineral to the concentration in the rock). There the accessories and the secondary epidote minerals are crucial for the whole *REE* balance. It is worth noting that the contribution of biotite to the bulk *REE* balance is lower in comparison to the biotite from the equigranular granitoids.

The most noteworthy characteristics of the ORG-normalized diagrammes of selected representative samples (Fig. 21) are their similarity with the calc-alkaline orogenic granites (Pearce et al. 1984). The patterns of all rock units demonstrate similarities with the arc magmas, but also with the collisional and post-collisional settings in being predominantly

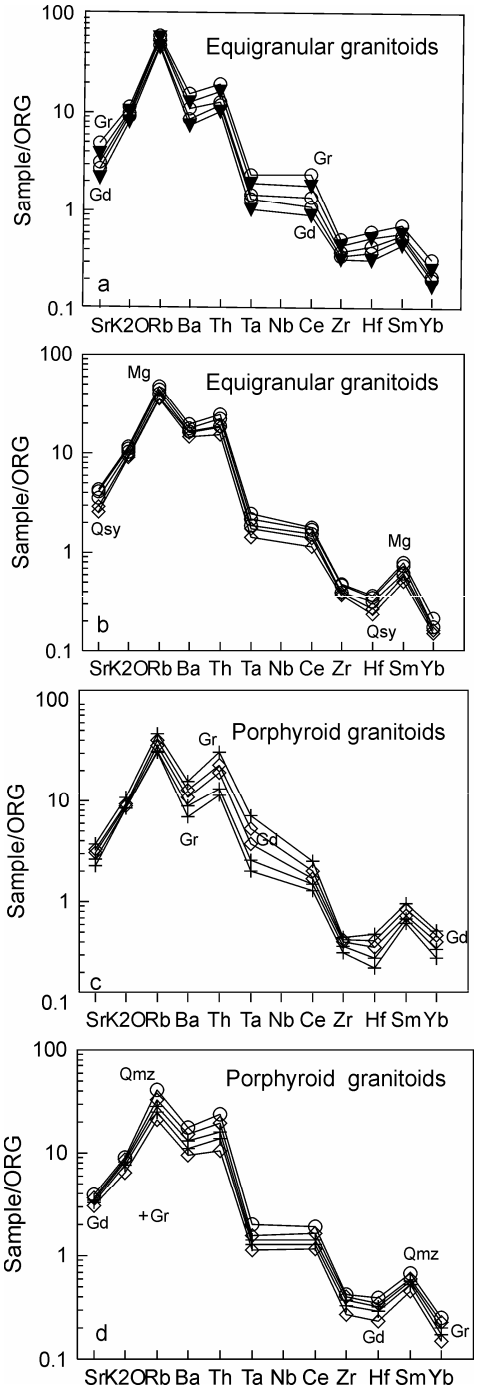

Fig. 21. ORG-normalized multi-element patterns for representative samples from the batholiths

LILE (K, Ba, Rb and Th) enriched and *HFSE* (Ta, Ce, Zr, Hf, Sm and Yb) depleted. No significant distinctions between the equigranular and the porphyroid granitoids are established in their spidergrammes. Small differences are found in the equigranular granitoids between the patterns of the modal granodiorite and granite (Fig. 21a) and the patterns of the transitional in alkalinity quartz-syenite and monzogranite (Fig. 21b). The former display a bit deeper negative Ba-anomaly and relatively higher normalized values of Ce at the background of the lower Ce, while the second modal species with higher transitional alkalinity shows patterns with increased normalized values of Ba, Ta and Sm and weakly decreasing Ce and Hf values. Similar differences are repeated at the analogous modal varieties of the porphyroid granitoids (Fig. 21c – normal calc-alkaline granodiorites and granites and Fig. 21d – transitional granodiorites and quartz-monzonites with higher alkalinity). The aplitoid granites (Fig. 22a-c) are distinguished by their reduced normalized values for Sr, Rb, Ba, Th, Ce and Zr and higher values of Ta. There however, the negative Ta-anomaly is replaced with a hint of a weak positive anomaly. The depletion of these elements in the acid magmatic residuum melts is a usual characteristic for the aplitoid rocks because they have already been fixed in their larger part in the other earlier granitoids. Several differing patterns of normalized distributions can be distinguished in this rock unit. The first of these models (Fig. 22a) has a bifurcate part of the spidergrams with preserved positive anomalies at Rb and Th and negative at Ba, but with deeper normalized values for Ba and significantly lower at Th. The slight humpy part at Ta is a characteristic difference from the subduction-related settings. This sort of patterns shows also differences between the leucogranites and the transitional alkaline granites, the last ones being with a more fractionated models, clearer expressed Sm-positive anomaly and distinctly higher contributions of Ta. The leucogranites are

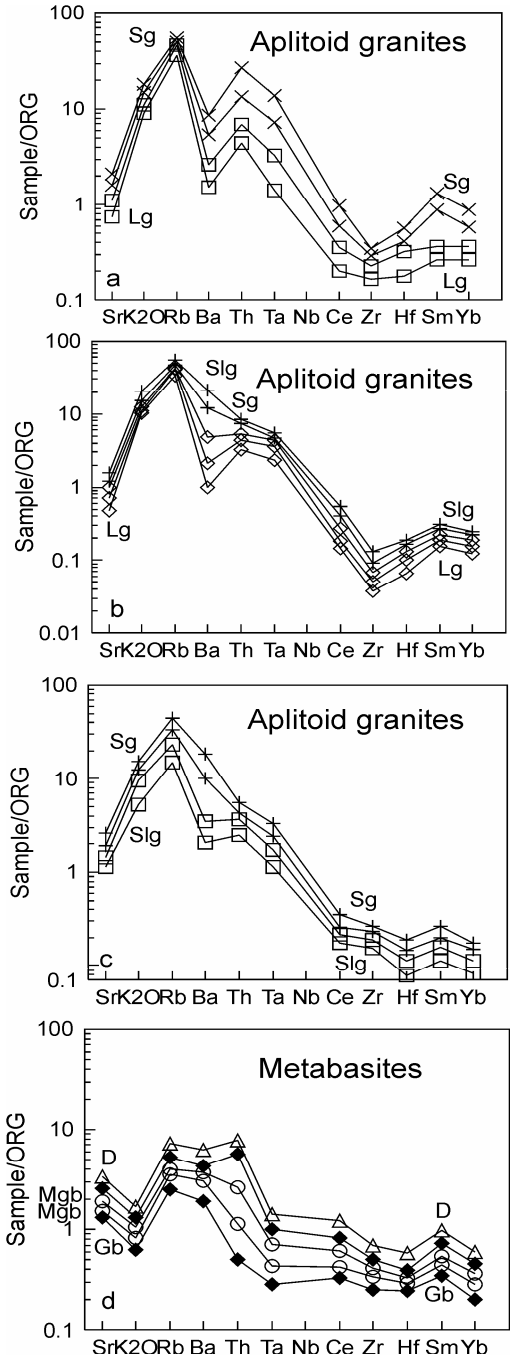

Fig. 22. ORG-normalized multi-element patterns (after Pearce et al. 1984) for representative samples from the batholiths

stronger depleted in all trace elements and especially in Sm, their normalized value lacking the above positive anomaly. The second model (Fig. 22b) is with still stronger depletion in Zr, Hf and Yb, but with preserved positive Sm-anomaly. Both modifications of the trace-element distributions noted above are also expressed clearly. The leucogranites are more depleted of all trace-elements and the difference from the transitional in alkalinity leucogranites and granites is mainly in the normalized concentrations of Ba, which is higher in the last rock varieties. The third type of models (Fig. 22c) is typical for the transitional in alkalinity leucogranites and granites. The normalized Th concentrations are lower, which leads to the disappearance of the positive peak at Th, as well as to negative anomaly at Zr. At the same time a characteristic negative anomaly at Hf appears. Both modifications distinguished above for the other models in the aplitoid granites are outlined here again. The higher normalized values at Ba in the transitional in alkalinity granites are an essential feature leading to the disappearance of the negative Ba-anomaly, so typical for the leucogranites.

The alkalinity of the rocks could be expressed also with the ratio Ta/Hf having the same geochemical significance as the ratio Nb/Y used by Pearce (1982) for discriminations. On Fig. 23a this ratio Ta/Hf is compared to SiO_2. The higher alkalinity of the aplitoid granites (3) is obvious as compared to the other rock varieties as well as the indiscernible under these framework rocks of the equigranular (1) and porphyroid (2) granitoids. However, if this measure of alkalinity Ta/Hf ratio is compared with the concentrations of Ba (Fig. 23b), in addition to the already manifested higher Ta concentrations in the aplitoid granites, another possibility for distinguishing of both differing geochemical subgroups can be found. The poorer in Ba aplitoid leucogranites (3a) and the richer in Ba transitional in alkalinity granites and leucogranites (3b) are clearly demarcated. The samples from the amphibolite xenoliths are

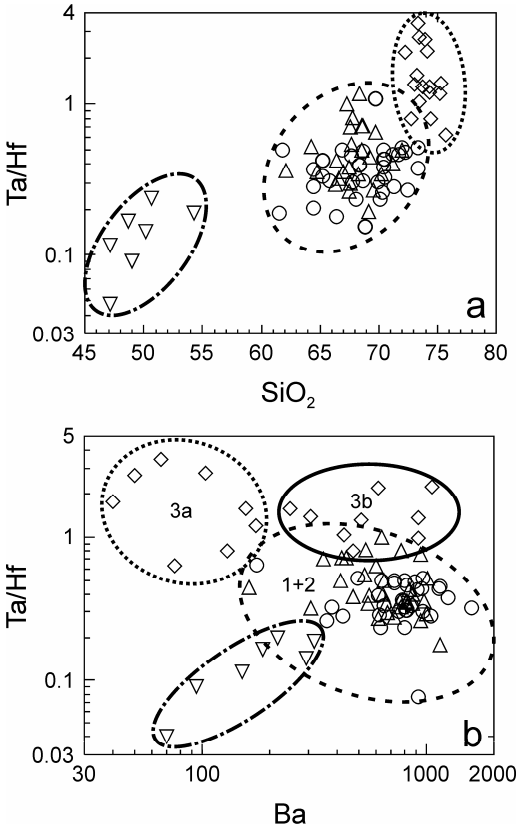

Fig. 23. Diagrams alkalinity (Ta/Hf) *vs.* SiO2 (a) and Ta/Hf *vs.* Ba (b). Solid ellipse: transitional granites and leucogranites

also plotted on the same diagramme and they display specific character (4).

The trace-element evolution in the magmatic rocks can be traced out on the log-log diagramme (Cocherie 1986) comparing the concentrations of a high-compatible component (TiO_2 in the case) against a high-incompatible component (here K_2O). Fig. 24 is the graphic expression of these relationships. Fractional crystallization is the only differentiation process, which causes trace elements to follow a Rayleigh distillation pattern, defining straight lines with steep slopes. It follows that the residual liquids of the leucogranites are mostly a result of fractional crystallization of an intermediate parental magma and all deviations out of the linear strip are inconsistent with the fractionation and owe their position to other processes. Thus, part of the porphyroid granitoid samples is displaced to the direction of the vector of decreasing K_2O values. The logical explanation is that the mobilization of K_2O during the re-crystallization (related to the growth of phenocrysts) is responsible for this peculiarity. Probably the locally superimposed albitization also influenced these deviations. It seems that the formation of the aplitoid granites was controlled by two factors because their samples on the diagramme fall into two fields, corresponding well to the deduced-above two differing modifications in their ORG-normalized patterns. The first field of the aplitoid granites (3a) is a natural extension of the fractional crystallization process and the second one (3b) is significantly deviated as a result of fluid impact. The last samples are typical transitional in alkalinity granites and leucogranites having also a wide range of the ratios Ba/Th (a measure of the fluid influence on magmatic differentiation).

Tectonic discriminations

Unequivocal discrimination of the geodynamic setting does not follow from the ORG-normalized patterns. The results of application of De La Roch et al. (1980) discrimination are also mixed. The samples from Sakar batholith plot in the fields of the plate margin magmatic series, in the post-collisional and late-orogenic granitoids.

On the Ta *vs*. Yb (Fig. 25a) diagramme after Pearce et al. (1984) the rocks from the batholith bear the geochemical characteristics of volcanic-arc and syn-collisional setting and even part of them plot in the field of the within-plate granites. Nearly the same are the results of the Rb *vs.* SiO_2 discrimination plot (not shown), where the main part of the samples occupies the field of volcanic arc granites and only a small part of them is in the field of syn-collisional granites. In the discrimination diagramme Rb *vs.* Yb+Ta (Fig. 25b) the

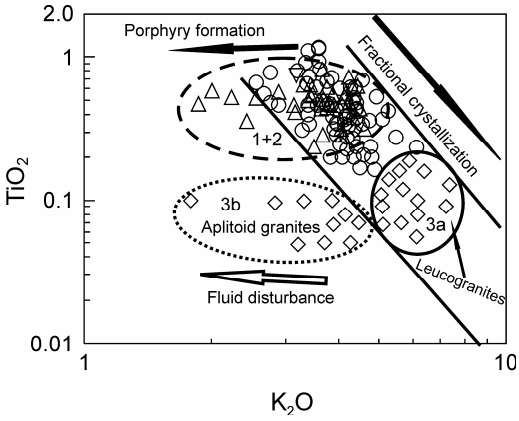

Fig. 24. Log TiO_2 *vs*. log K_2O plot (after Cocherie 1986) for rocks of the batholith

prevailing number of samples is in the field of volcanic-arc granites and only an insignificant amount of samples falls within the fields of syn-collisional granites and the within-plate granites. The reasons for the unsuccessful discriminations are due to the fact that the fractionation between the liquidus and solidus phases could have been imperfect due to the high viscosity of the acid magmas. Some of the plagioclase or potassium feldspar crystals probably could not fractionate fully and remained within the solidifying magmas, thus displacing the samples to the field of the volcanic arc granites. The influx of volatile components bearing also Ta has exported many of the other trace-elements. This could be a likely reason for the deviations in the fields of the within-plate granites.

The plot after Harris et al. (1986) Rb/Zr *vs.* SiO_2 (Fig. 25c) implies that syn-collisional setting may be assumed only for part of the aplitoid granites that were probably influenced by fluid-related differentiation. The discrimination diagramme Hf-Ta-Rb on Fig. 25d allows assuming a mixed geochemical characteristic for the equigranular and for the porphyroid granitoids – volcanic arc and late-/post-collisional granites. The leucocratic and aplitoid unit should be excluded from the discrimination owing to the strong fluid impact during their formation. It may be assumed that the parental magma had a mantle source but was subjected to widely developed contamination with crustal materials. The only one more conclusive piece of evidence for the post-collisional setting is the relatively increased Ta abundances in the rocks, having shallower negative Ta-anomalies in the ORG-normalized patterns.

Discussion

The origin of the granitoid magma is debatable for lack of sufficient modern and more precise isotopic data. The initial $^{87}Sr/^{86}Sr$ ratios from different combinations of bulk rock samples vary in a wide range – from 0.7029 (Lilov 1990) or 0.7056 (Zagorchev et al. 1989) to 0.708 (Skenderov & Skenderova 1995) and their interpretation in a plausible way is next to impossible.

The petrographic features of the granitoids tentatively suggest that most probably the parental magma derived from melting of lower crust materials implying a source with mixed mantle-crust geochemical characteristics. The over-clarkes concentrations of the trace elements Sc, Mo, Ni and V and the bellow-clarkes amounts of Rb, Li, Cs, Zr and *REE* in the rocks could be a geochemical fingerprint of the mantle/or lower crust component in the composition of their magma source. The supposed petrographic composition of such a source should be similar to the composition of the orthoamphibolites, so often met in the batholith. The orthoamphibolites might pertain to gabbro, monzogabbro, diorite and monzodiorite judging from the relations in the TAS diagramme. Their samples form a characteristic bifurcate field in the serial diagramme K_2O *vs.* SiO_2 (Peccerillo & Taylor 1976 with the extension of Dabovski et al. 1991). One of the branches falls in the tholeiite and the calc-alkaline series and the second one cuts steeply all series and reaches up to the shoshonite series (Fig. 26). The last trend reflects the redistributions of mobile components in the

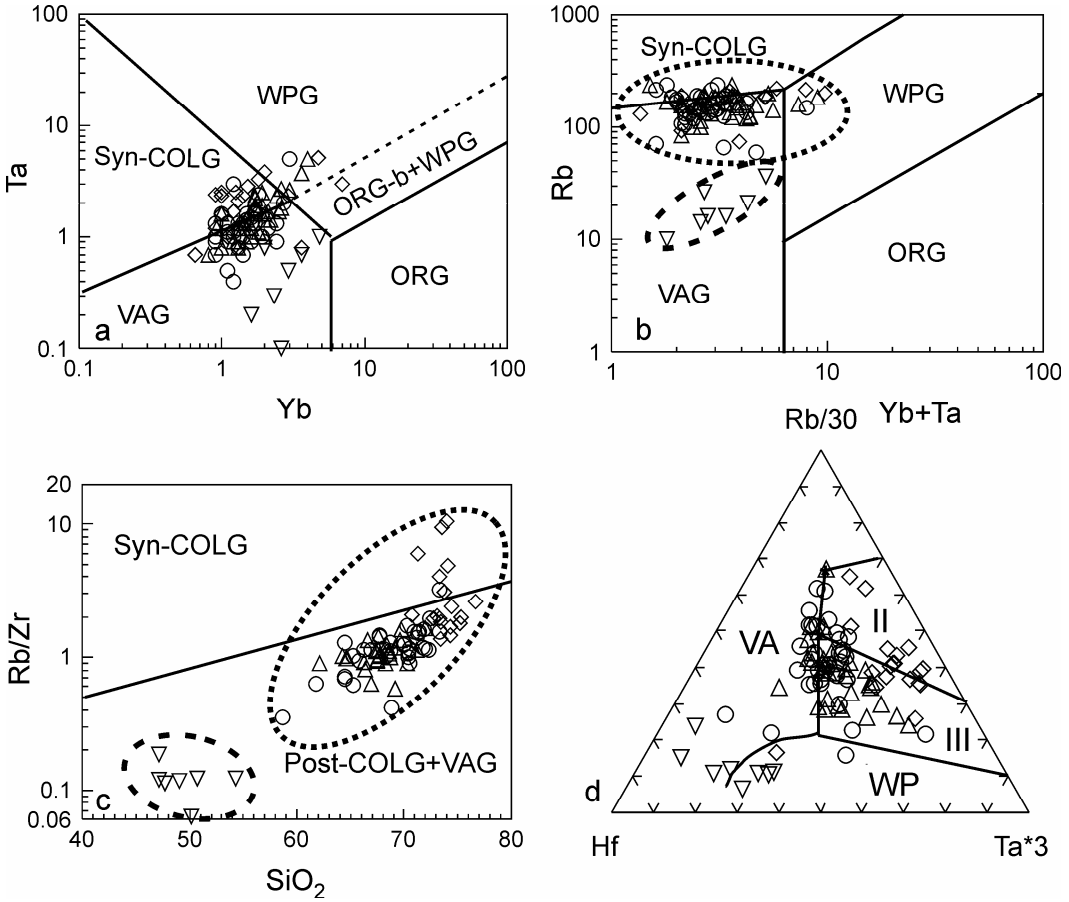

Fig. 25. Discrimination diagrammes for rocks of the batholith. a) Ta *vs.* Tb after Pearce et al. (1984); b) Yb+Ta *vs.* Rb after Pearce et al. (1984); c) SiO_2 *vs.* Rb/Zr after Harris et al. (1986); d) Rb/30-Hf-Ta*3 after Harris et al. (1986). Fields: (Syn-COLG) syn-collision peraluminous granites; (WPG) within-plate granites; (ORG) ocean-ridge granites; (VAG) volcanic-arc granites; (Post-COLG) post-collision granites; (II) syn-collision peraluminous leucogranites; (III) late or post-collision granites

course of the alterations and is related with the stronger expression of the granitization process that led to the increase of the K_2O contents. Similar two-branched distributions are established in some of their Harker's plots as for example the ones of P_2O_5 and MgO. It becomes clear that the granitization was related to relative decrease of MgO and input of P_2O_5. The magma of the orthoamphibolites was typical metaluminous (Figs. 10, 11). In view of their basic composition, the orthoamphibolites could be perceived as metamorphosed earlier parental products of the granitoid magma because their fields in some geochemical diagrammes are connected in common trends with the fields of the granitoids from the batholith (Figs. 14, 23a), but there are essential differences in the distributions of their trace elements. Thus, for example, orthoamphibolites are far from geochemically similar with the granitoids in their relationships between Ba and Sr, in the range of the ratios Ta/Hf (Fig. 23b) or of the ratios Ce/Th and the search of a direct magmatic relation was unsuccessful. The

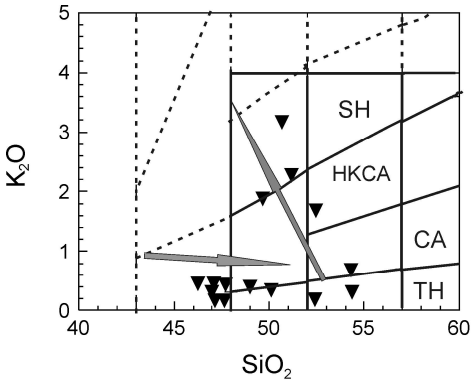

Fig. 26. SiO_2 *vs.* K_2O plot (Peccerillo & Taylor 1976) extended along the hatch-lines by Dabovski et al. (1989) for orthoamphibolites from the Sakar batholith. Arrows: chemical trends

differences with the granitoids are especially distinctive in the ORG-normalized models (Fig. 22d) where the enrichment of *LILE* is weaker and a typical minimum at the place of K_2O is established. All elements from Ta to Yb are without the typical for the granitoids strong depletion related to the standard and to *LIL* elements. Some differentiation in the protoliths of the orthoamphibolites in the sequence gabbro–monzogabbro–diorite become apparent following the consecutive increase of the normalized concentrations of Th, Ce and Sm. Chondrite-normalized *REE* patterns (Fig. 18c) display the typical for basic rocks distribution without enrichments in the *LREE* part, much shallower negative Eu-anomalies and a negative Lu-anomaly different from the patterns of equigranular and porphyroid granitoids (Fig. 17). The geochemical discriminations after De La Roch (1980) and the other methods applied (Fig. 25) undoubtedly point to a volcanic arc origin of the basic magma. Probably, such was the setting of the lower crust amphibolite source – one of the components of the granitoid parental magma. This setting was imprinted on the volcanic arc characteristics of part of the granitoid samples, which are discriminated with ambiguity.

The evaluation of physical parameters during the generation and cooling of the granitoids is important, but the available tools are scanty. Partial melting of tonalitic rocks, similar to the orthoamphibolites in Sakar batholith is able to generate acid or intermediate parental magmas. Published experiments (Naney 1983; Piwinskii 1968; Skjerlie & Johnston 1993; Schmidt 1993) estimate such temperature range as 850-825°C at the pressure range of 5-8 kbar. The increased Rb and Ta contents in the granitoid melts in comparison with the depleted amphibolite source is a result of their incompatible behaviour in the melting process, but possibly can be also a consequence of the contributions from the upper crust. Thus, the mixed mantle-crust magma composition can explain why the samples plot into the fields of volcanic arc and post-collisional settings.

The oxidizing conditions of crystallization are estimated by the application of the method of Wones & Eugster (1965). All analyzed biotites fall around the buffer magnetite-hematite (HM) or between the buffers HM and NNO (Ni-NiO), which defines rather high pO_2 during their crystallization. There are some cases of biotites even exceeding this buffer. The registered consecutive increase of the oxidation degree in the magmas of the later granitoids is indicative for almost attained water saturation at the latest acid magmas. This conclusion is supported by the presence of graphic textures in the aplitoid granites.

The occurrence of allanite in the granitoids from Sakar batholith is a function partly by magma composition and partly by the depth of crystallization. At temperatures above the water saturated solidus the stability of epidote (and of allanite as being *LREE*-enriched epidote) strongly depends on fO_2 (Schmidt & Thompson 1996). More oxidizing conditions favor greater temperature and thus lower pressures. The intersection of the solidus-epidote dehydratation at fO_2 between HM and NNO buffers with the water-saturated tonalite solidus is located at a pressure range 3-5 kbar. These experimental data confirm the minimum pressure required for allanite formation in Sakar granitoids. The lower limit

is more probable because fO_2 is buffered at higher value in some cases (e.g. HM in some of the biotites, Fig. 6). This estimation of the pressure is comparable with the minimum pressure of the co-crystallization of biotite and muscovite – 3.4 kbar (Kistler et al. 1981) evaluated by means of the intersection of the stability curve of the association muscovite + quartz with the solidus of the water-saturated granite. Probably this barometric estimation should be questioned because of the widespread subsolidus re-equilibration of muscovite, but generally the similar results for the crystallization of the allanite are significant.

Applying the *LREE* saturation in felsic melts with SiO_2 ~ 73 wt.% we may evaluate the crystallization temperature roughly (Watt & Harley 1993). The obtained results are in the range 730–800°C for the equigranular and porphyroid granitoids and 600–700°C – for the aplitoid granitoids. Almost the same are the estimations when the method of Watson & Harrison (1983) of the zircon saturation effects on temperature and compositions of acid melts is exercised. Additional consequence is that most of the zircons from the Sakar granitoids are inherited from their country rocks.

The high ordering degree of the microclines in the rocks corresponds both to the advanced erosion and to the mesozonal facies of the batholith, where the fluid pressure was sufficiently high. The correlation between the amount of Al atoms in the site T_1O and the temperature at the stopping of the process of the ordering (Stewart & Wright 1974) in the microclines is used to estimate the crystallization temperature. The obtained temperatures of microclines from the equigranular granitoids are 540–420°C and for the microclines from the porphyroid granitoids – 585–450°C. Comparable temperatures are obtained applying the geothermometer of Stormer (1975) based on the model of distribution equilibrium of the co-crystallizing plagioclase and potassium feldspar under 5 kbar pressures. The results support the idea that the equilibration of the potassium feldspars was accomplished in relatively water rich conditions.

The variety of the rocks in Sakar batholith may be explained by fractionation of an intermediate partial melt, but contaminated with upper crust materials and accompanying fluid differentiation, more intensive during the latest stages of magma evolution. The parental magmas were primarily rich in water and fluids, and had high potential of their alkalies. The experimental data (Holtz et al. 1992) may help in understanding the modal tendencies. The modal trend 1 (Fig. 3) could be a result of normal polybaric fractional crystallization in the equigranular granitoids. The modal trend 2 is related to almost constant water activity (aH_2O) during the crystallization, but with increased activity of the alkali components in the trans-magmatic fluxes, provoked the porphyroid formation. The modal trend 3 of the aplitoid granites indicates almost isobaric crystal fractionation of quartz and feldspar phases in the residuum magma, leading to progressive enrichment of the melt with water. The following observations witness high water pressure: the wealth of aplitic and pegmatitic veins accompanying the granitoids, the occurrence of muscovite with features of primary magmatic origin, the exceptional poorness of magnetite in the rocks, the relatively low content of FeO and K_2O in the plagioclases, etc.

All obtained estimations for the physical parameters during generation and crystallization of the granitoid magmas in Sakar batholith lead to the conclusion that the parental magma of the pluton has been generated at depths of about 13–15 km and transported to depths of 8–9 km, where fractionated and partly solidified. The crystallization was continuing in the rising melt and reached the water-saturated conditions in its final stages. The estimated crystallization temperatures for the Sakar granitoids characterize them as "cold granites" (Miller et al. 2003).

The origin of potassium feldspar porphyries in the rocks is late-/or postmagmatic. The porphyry formation is related to transmagmatic solutions with transitional characteristics between diffusion and infiltration fluxes, according to the ideas of Korzhinskii (1953).

These solutions, rich in water vapor and potassium ions, form in the peripheral zones of the granitoid pluton and penetrate into the country rocks. The export of potassium ions forms areas with locally low K_2O concentrations and this favours the growth of potassium feldspar endoblasts, owing to dissolution of the fine-grained microclines and their re-crystallization into large crystals. Field observations show an alternation of strips strongly enriched in microcline porphyroids and others with very rare porphyroids, which are parallel to the contact surfaces of the pluton. The thickness of such strips is of the order of 5 to 10 m. Most likely these zones within the porphyroid granitoids reflect periodical changes in the concentration gradients of potassium ions. Later, the growing by re-crystallization large microclines suffered re-orientation caused by shear zones or pericontact and regional deformations. According to the logics of the accepted model for porphyroid formation, the infiltration fluxes rich in K_2O should fix the latter in exoblastic potassium feldspars growing in the host rocks. Large-sized microclines found in the meta-granites around Izvorovo village (Fig. 1) probably have such an origin. Previously these rocks have been mapped as classical regional migmatites. It is significant that the porphyroblasts of the zones of exocontact microcline growth have the same structural features and the same microchemical composition as the feldspars of the aplitoid or pegmatite residuum of the rich in vapor acid-alkali granite magma.

The emplacement of the main phase of the equaligranular and porphyroid granitoids can be explained by the "balloon mechanism". In the course of the consecutive intrusion of new portions of magma into the central parts of the dome, the older more or less consolidated batches were stretching and inflating like balloon and deformed in the same way as metamorphic rocks. In this way originated structures resembling crystallization schistosity, lenticular enclaves, deformed feldspars and elongated quartz aggregates. This sort of deformations is syn-intrusive and occurred before the emplacement of the aplitoid granites and leucogranites, aplites and pegmatites, which were not affected by the deformations. The imposed albitization is not reliably dated. It can be much later than the crystallization of the batholith, maybe post-Triassic, because albitization is established also in the low-grade metamorphic Triassic sediments.

Conclusions

The Sakar batholith consists of three granitoid units: equigranular, porphyroid and aplitoid. The modal petrographic varieties in the first two units are quartz-monzodiorite, quartz-monzonite, granodiorite, monzogranite, and in the aplitoid granitoids – leucogranodiorite, leucogranite and granosyenite. Indications for late-magmatic to post-magmatic re-crystallization and porphyroblastic growth of microcline are established as well as traces of superimposed deformation and metamorphic processes.

Plagioclases are fully to partially structurally ordered and occur as two morphological types, distinguished by their zonal patterns. According to anorthite composition and trace-element concentrations, the difference between plagioclases from the equaligranular and porphyroid granitoids is unessential. The potassium feldspars are high ordered microcline-microperthite. However, there are some distinctions between their trace-element compositions, depending on the affiliation to a specific rock unit. Zonal distribution of some trace-elements in their crystals is typical. There are also traces of late- or post-magmatic re-crystallization, related to the fluid evolution of the batholith. Biotites also show specific features for different rock units. Muscovites are of magmatic and of post-magmatic types. Among the accessories, titanite and allanite are typical.

The composition of minerals provides a possibility to estimate the physical-chemical crystallization conditions – moderate depth, low temperatures, high potential of water and oxygen, slightly increased alkalinity of the magmas. The parental magma was of calc-alkaline affinity.

The most likely magma source contained lower crust materials and the mantle component in the rocks was probably inherited from this source. Upper crust contamination was essential.

The discriminations determine mixed geochemical characteristics, indicating volcanic arc and late-/or post-collisional settings. We assume that the last one is more realistic due to the somewhat increased Ta concentrations in the rocks. The partial magmas were products of fractional crystallization, fluid impact and assim-ilation phenomena that generated metaluminous and peraluminous rock varieties. Part of the deformations in the batholith is interpreted by the "balloon mechanism" of emplacement.

The obtained new petrological and geochemical data, together with the speculations for their origin, could be a basis for future comparative detailed studies on other Late Paleozoic acid intrusions in Bulgaria.

Acknowledgements: Part of this study was financially supported by the former enterprise "Rare metals" (Geological Prospecting Department) under Contract 154/82. S. Savov and I. Genov took part in some of the fieldwork. Particular traverses were made together with geologists of the above-mentioned enterprise I. Palshin, G. Skenderov, and D. Petev. We thank the help and consultations of V. Arnaudov and R. Arnaudova during the sample processing of artificial heavy concentrates. We are grateful also to A. Andreev who advised the statistical calculations of the data and to V. Neichev and L. Christov for their help in the monomineral separation of the samples.

References

Abdel-Rahman A-FM (1994) Nature of biotites from alkaline, calc-alkaline and peraluminous magmas. *Journal of Petrology*, **35**, 525–529

Arnaudov V (1979) "South Bulgarian granites" – controversial problems. *Geologica Balcanica*, **10**, 1, 29–32 (in Russian)

Arnaudova R, Arnaudov V (1982) Comparative geochemistry and conditions of formation of the "South Bulgarian granites". *Geologica Balcanica*, **12**, 4, 21–36 (in Russian)

Arnaudova R, Pavlova M, Arnaudov V (1981) Distribution of iron in plagioclases from the "South Bulgarian granites". *Review of the Bulgarian Geological Society*, **42**, 2, 257–261 (in Bulgarian)

Arnaudova R, Cherneva Z, Stancheva E (1990) Structural state and geochemical characteristics of potassic feldspars from the Central Rhodope metamorphic complex. *Geologica Balcanica*, **20**, 1, 67–84

Boyadjiev S, Lilov P (1972) On the K-Ar dating of the South Bulgarian granitoids from Srednogorie and Sakar-Strandja Zones. *Proceedings of the Geological Institute, ser. Geochemistry, Mineralogy, Petrography*, **26**, 2, 121–220 (in Bulgarian)

Boyanov I, Kozhoukharov D, Savov S (1965) Geological structure of the southern slope of Sakar Mountain between the villages Radovets and Kostur. *Review of the Bulgarian Geological Society*, **26**, 2, 121–134 (in Bulgarian)

Čatalov G (1961) Triassische kristalline Schiefer und Magmagesteine zwischen Haskovo und Dimitrovgrad. *C.R. Acad. Bulg. Sci*., **14**, 5, 503–506

Chatalov A (1992) Petrological peculiarities of the rocks from the Melnik orthometamorphic complex, Sakar Mountain. *Review of the Bulgarian Geological Society*, **53**, 3, 99–112 (in Bulgarian)

Chatalov G (1990) *Geology of the Strandja Zone in Bulgaria*. Bulgarian Academy of Sciences Press, Sofia, 263 p. (in Bulgarian)

Cocherie A (1986) Systematic use of trace element distribution on patterns in log-log diagrams. *Geochimica et Cosmoshimica Acta*, **50**, 2517–2522

Cullers RL, Graf JL (1984) Rare earth elements in igneous rocks of the continental crust: Intermediate and silicic rocks and their petrogenesis. *Rare Earth Element Geochemistry*. Elsevier, 275–308

Dabovski C (1968) Paleozoic magmatism. Formation of the South Bulgarian granitoids. In: Tsankov V, Spasov C (Editors) *Stratigraphy of Bulgaria*, p. 121–134, Nauka and Izkustvo, Sofia (in Bulgarian)

Dabovski C, Haidutov I (1980) The Sakar pluton. In: Kozhoukharov D, Dabovski Ch (Editors) *The Precambrian in south Bulgaria*, Guide to excursion IGCP Project 22, Bulgaria, October 1980, Bulgarian Academy of Sciences, Geological Institute, 83–89

Dabovski C, Harkovska A, Kamenov B, Mavrudchiev B, Stanisheva-Vassileva G, Yanev Y (1991) A

geodynamic model of the Alpine magmatism in Bulgaria. *Geologica Balcanica*, **21**, 4, 3–15

De La Roch H, Leterrier J, Grandclaude P, Marshal M (1980) A classification of volcanic and plutonic rocks using R_1-R_2 diagrams and major element analyses – its relationships with current nomenclature. *Chemical Geology*, **29**, 183–210

Dimitrov I (1999) Internal structure of the metagranitoids in the Sakar region, SE Bulgaria. *Geologica Balcanica*, **29**, 111–124

Dimitrov S (1946) The metamorphic and magmatic rocks in Bulgaria. *Annual of the Direction of Geological and Mining Prospecting*, A, **4**, 61–93 (in Bulgarian)

Dimitrov S (1956) Die kinetische Regionalmetamorphose der Jurassischen Ablagerungen und Leucogranite in Süd-Ost Bulgarien. *Abhandlungen des XX Intern. Geol. Kongr. in Mexico*, 327-333

Dimitrov S (1959) Kurze Übersicht der metamorphen Komplexe in Bulgarien. *Freiberger Forschungshefte*, Reih, C., H. **57**, 62-72

Efremova SV, Stafeev KG (1985) *Petrochemical Methods in Studying Rocks*. Nedra, Moscow, 511 p. (in Russian)

Firsov L (1975) On the age of South-Bulgarian granites in the Rhodopes, Srednogorie and Sakar-Strandja areas. *Geology and Geophysics*, **1**, 27–34 (in Russian)

Gerdjikov I (2005) Alpine metamorphism and granitoid magmatism in the Strandja zone: New data from the Sakar unit, SE Bulgaria. *Turkish Journal of Earth Sciences*, **14**, 167–183

Gerdjikov I, Ivanov Z (2000) Main features of pre-Tertiary basement of the Maritza area. *Annuaire de L'Universite de Sofia, "St. Kliment Ohridski", Faculte de Geologie et Geographie,* livre 1, Geologie, **92**, 13–21

Georgiev SV, von Quadt A, Heinrich CA, Peytcheva I (2006) Geochemistry and U-Pb dating of the magmatism in Eastern Srednogorie, SE Europe. *Joint assembly AGU, G, MAS, SEG and UGM, Baltimore,* MD, V41A-20

Grancharov C, Belmustakova H, Arnaudova R (1979) Structural types potassium feldspars from the Gutsal and Varshilo granitoids (Ihtiman Sredna Gora). *Review of the Bulgarian Geological Society*, **40**, 2, 185–189 (in Bulgarian)

Harris N, Pearce JA, Tindle A (1986) Geochemical characteristics of collision-zone magmatism. In: Coward MA, Ribbe PH (Editors), *Collision tectonics, Geol. Soc. Spec. Publ*., **19**, 67–81

Holtz F, Pichavant M, Barbey P, Johannes W (1992) Effects of volatiles on mixing in calc-alkaline magma systems. *American Mineralogist*, **77**, 1223–1241

Ivanov I (1964) The metamorphosed porphyry granites between the villages Bulgarin and Shishmanovo, District Harmanli. *Review of the Bulgarian Geological Society*, **30**, 3, 229–238 (in Bulgarian)

Ivanov Z, Gerdjikov I, Kunov A (2001) New data and considerations about the structure and tectonic evolution of Sakar region, South-East Bulgaria. *Annuaire de L'Universite de Sofia, "St. Kliment Ohridski", Faculte de Geologie et Geographie,* livre 1, Geologie, t. **91**, 35–80 (in Bulgarian)

Kamenov B, Vergilov V, Genov I, Vergilov I, Savov S, Dabovski C, Ivchinova L (1986) Geological structure and petrographical peculiarities of the Lessovo orthometamorphic complex. *Strandja-Sakar Collection*, Yambol, **IV**, 8, 145–157 (in Bulgarian)

Kistler RW, Ghent ED, O'Neil JR (1981) Petrogenesis of garnet two-mica granites in the Ruby Mountains, Nevada. *Journal of Geophysical Research,* **86**, 10591–10606

Kozhoukharov D (1984) Litostratigraphy of Precambrian metamorphic rocks of the Rhodope Supergroup in the Central Rhodopes. *Geologica Balcanica*, **14**, 1, 43–92 (in Russian)

Kozhoukharov D, Savov S, Chatalov G, Kozhoukharova E., Boyanov I, Chelebiev E (1994) *Explanatory note to 1:100 000 Map Sheet Topolovgrad.* Sofia, Commitee of Geology and Mineral Resources, Geology and Geophysics, 73 p. (in Bulgarian)

Kozhoukharov D, Boyanov I, Kozhoukharova E, Goranov A, Savov S, Shilyafov G (1995) *Explanatory note to 1:100 000 Map Sheet Svilengrad.* Sofia, Commitee of Geology and Mineral Resources, Geology and Geophysics, 67 p. (in Bulgarian)

Kozhoukharov D, Boyanov I, Savov S (1968) Geology of the area between village Klokotnitsa and Maritsa town, Haskovo District. *Jubilee Collection Geological Institute and Committee of Geology*, **32**, 12, 37–50 (in Bulgarian)

Kozhoukharova E, Kozhoukharov D (1973) Stratigraphy and Petrology of the Precambrian metamorphic rocks from Sakar Mountain. *Proceedings of the Geological Institute of the Bulgarian Academy of Sciences*, **22**, 193–213 (in Bulgarian)

Korzhinskii DS (1953) Outline of the metasomatic processes. In: *Basic Problems of the Magmatic Ore Deposits*. Academy of Sciences USSR, Moscow, 268 p. (in Russian)

Kuznetsova LG (1970) Application of IR-spectroscopy for determination of the ordering degree of potassium feldspars. *Mineralogical Collection*, Lvov University, **25**, 1–10 (in Russian)

Kuznetsova LG, Stankevich EK, Tsentner ID (1974) Methods of IR-spectroscopy in the studies of the structural state in plagioclases. In: *Minerals and Paragenesis of Magmatic and Metasomatic Rocks*, Nauka, Leningrad, 50–60 (in Russian)

Laves F, Goldschmidt VM (1956) Distal and close order of the basic plagioclases at continuous and inverse temperature function. In: *Feldspars*, **2**, Leningrad, 68–86 (in Russian)

Lilov P (1990) Rb-Sr and K-Ar dating of the Sakar granitoid pluton. *Geologica Balcanica*, **20**, 6, 53–60 (in Russian)

Marakushev A, Tararin I (1965) Mineralogical criteria of the alkalinity of the granitoids. *Proceedings of the Academy of Sciences of USSR*, ser. Geochemistry, **3**, 20–37 (in Russian)

Miller CF, Meschter-McDowell S, Mapes RW (2003) Hot ad cold granites? Implications of zircon saturation temperatures and preservation of inheritance. *Geology*, **31**, 529–532

Monier G, Daniel JM, Labernadiere H (1984) Generations successive de muscovites et feldspars potassique dans les leucogranite du massif de Millevaches (Massif Central Francais). *Bulletin Mineralogie*, **107**, 55–68

Naney MT (1983) Phase equilibria of rock-forming ferromagnesian silicates in granitic systems. *American Journal of Science*, **283**, 993–1033

Palshin I, Skenderov G, Bojkov I, Michailov Y, Kotov E, Bedrinov I, Ivanov I (1989) New geochronological data for the Cimmeridian and Alpine magmatic and hydrothermal products in the Srednogorie and Stara Planina Zones in Bulgaria. *Review of the Bulgarian Geological Society*, **50**, 2, 75–92 (in Bulgarian)

Pearce JA (1982) Trace element characteristics of lava from destructive plate boundaries. In: Thorpe RS (Editor) *Andesites: Orogenic and Related Rocks*, Wiley, Chichester, New York, 525–548

Pearce JA, Harris NB, Tindle AG (1984) Trace element discrimination diagrams for the tectonic interpretation of granitic rocks. *Journal of Petrology*, **25**, 4, 956–983

Peccerillo A, Taylor SR (1976) Geochemistry of Eocene calc-alkaline volcanic rocks from the Kastamonu area, Northern Turkey. *Contributions to Mineralogy and Petrol*ogy, **58**, 63–81

Piwinskii AJ (1968) Experimental studies of igneous rock series, central Sierra Nevada batholith, California: Part II. *Neues Jahrbuch für Mineralogie*, **5**, 193–215

Plyusnina II, Hachatryan GK (1980) Investigations of the plagioclase composition and ordering degree by methods of IR-spectroscopy and diffractometry. *Order and Break Down of Solid Solutions in Minerals*. Nauka, Moscow, 27–38 (in Russian)

Sarafova N (1966) On some structural-optical types potassium feldspars from our old granitoids. *Papers on the Geology of Bulgaria, ser. Geochemistry, Mineralogy and Petrography*, **6**, 263–268 (in Bulgarian)

Savov S (1976) Lower Cambrian trace fossils from high-grade metamorphic schists, Strandja Mountain, South-East Bulgaria. *Paleontology, Stratigraphy and Lithology*, **5**, 19–22

Savov S (1983) Tectonics of the Oman portion of Northern Strandja Mountain and of part of the Bosna Dislocation Zone. *PhD thesis synopsis*, Bulgarian Academy of Sciences, United Centre of Earth Sciences, 40 p. (in Bulgarian)

Schmidt MW (1993) Phase relations and composition I tonalite as a function of pressure. An experimental study at 650^{o}C. *American Journal of Science*, **293**, 1011–1060

Schmidt MW, Thompson AB (1996) Epidote in calc-alkaline magmas: An experimental study of stability, phase relationships, and the role of epidote in magmatic evolution. *American Mineralogist*, **81**, 462–474

Skenderov G, Skenderova T (1995) Subduction of the Vardar oceanic crust at the end of Jurassic and its role for the Alpine tectonic-magmatic development of parts of the Balkan Peninsula. *Review of the Bulgarian Geological Society*, **56**, 2, 45–63 (in Russian)

Skenderov G, Palshin I, Michailov Y, Bojkov I, Savova L (1986) On the age of the Sakar granite pluton (South-Eastern Srednogorie). *Geochemistry, Mineralogy and Petrology*, **22**, 69–81 (in Russian)

Skjerlie KP, Johnston AD (1993) Fluid-absent melting behaviour of F-rich tonalitic gneiss at mid-crustal pressures: Implications for the generation of anorogenic granites. *Journal of Petrology*, **34**, 785–815

Speer JA (1984) Micas in igneous rocks. In: Bailey (Editor) *Reviews in Mineralogy*, **13**, 299–355

Stewart DB, Wright TL (1974) Al/Si order and symmetry of natural alkali feldspars, and the relationships of strained cell parameters to bulk composition. *Bull. Soc. Fr., Minéral., Crist*., **97**, 356–377

Stormer JCJr (1975) A practical two-feldspar geothermometer. *American Mineralogist*, **60**, 667–674

Vergilov V (1966) On the nature of sagenite in biotite. *C. R. Acad. bulg. Sci*., **19**, 7, 643–644

Vergilov V, Kamenov B, Dabovski C, Haydutov I, Genov I, Ivchinova L, Vergilov I, Andreev A (1986) New data on the Sakar batholith. *Strandja-Sakar Collection*, Yambol, **IV**, 8, 145–157 (in Bulgarian)

Watson EB, Harrison TM (1983) Zircon saturation revisited: Temperature and compositions effects in a variety of crustal magma types. *Earth and Planetary Science Letters*, **64**, 295–304

Watt GR, Harley SL (1993) Accessory phase controls on the geochemistry of crustal melts and restites during water-undersaturated partial melting. *Contributions to Mineralogy and Petrology*, **114**, 550–566

Wones DR, Eugster HP (1965) Stability of biotite: Experiment, theory and applications. *American Mineralogist*, **50**, 1228–1272

Wright TL (1968) X-ray and optical study of alkali feldspar. II. An X-ray method for determining the composition and structural state from measurement of 2 values for three reflections. *American Mineralogist*, **53**, 88–101

Zagorchev I, Lilov P, Moorbath S (1989) Rb-Sr and K-Ar radiogeochronological results on metamorphic and magmatic rocks from Southern Bulgaria. *Geologica Balcanica*, **19**, 3, 41–54 (in Russian)

Accepted April 14, 2009